



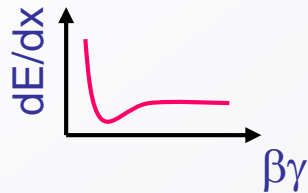
The Basics of Particle Detection

Christian Joram / CERN

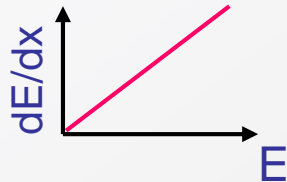
- **Lecture 1 – Interaction of charged particles**
- **Lecture 2 – Gaseous and solid state tracking detectors**
- **Lecture 3 – Calorimetry, scintillation and photodetection**
 - **Calorimetry**
 - electromagnetic cascades
 - hadronic interactions
 - neutrons and neutrinos
 - hadronic cascades
 - **Scintillation**
 - **Photodetection**

e^+ / e^-

- Ionisation

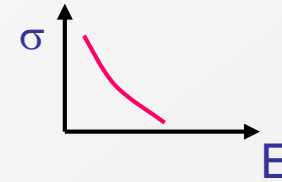


- Bremsstrahlung



γ

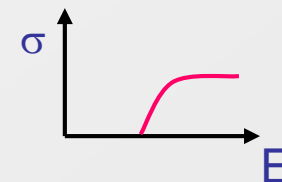
- Photoelectric effect



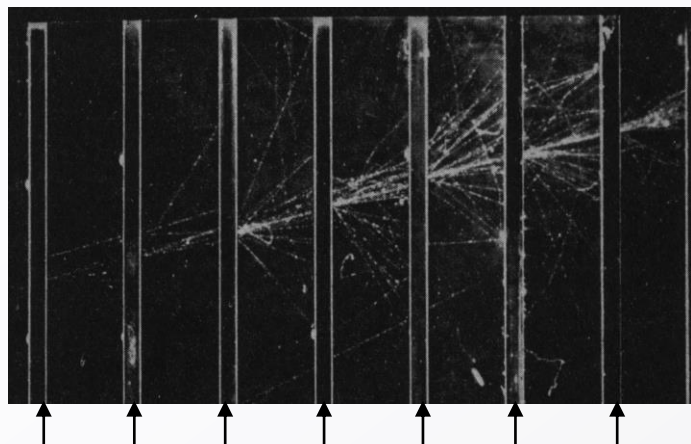
- Compton effect



- Pair production



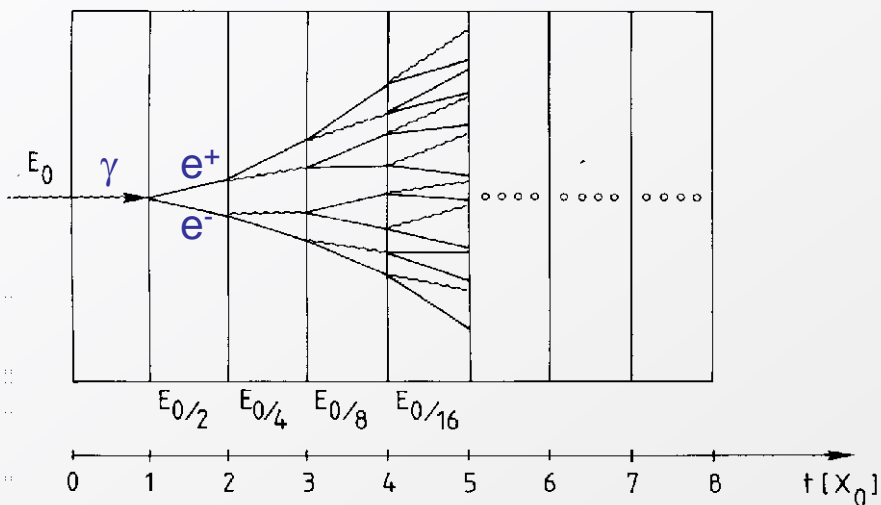
Electromagnetic cascades (showers)



← Electron shower in a cloud chamber with lead absorbers

Pb plates

Simple qualitative model



- Consider only **Bremsstrahlung** and (symmetric) **pair production**.
- Assume: $X_0 \sim \lambda_{\text{pair}}$

$$N(t) = 2^t \quad E(t) / \text{particle} = E_0 \cdot 2^{-t}$$

Process continues until $E(t) < E_c$

$$N^{\text{total}} = \sum_{t=0}^{t_{\text{max}}} 2^t = 2^{(t_{\text{max}}+1)} - 1 \approx 2 \cdot 2^{t_{\text{max}}} = 2 \frac{E_0}{E_c}$$

$$t_{\text{max}} = \frac{\ln E_0 / E_c}{\ln 2}$$

After $t = t_{\text{max}}$ the dominating processes are **ionization, Compton effect and photo effect** → absorption of energy.

Shower can be initiated by photon **OR** by electron.

- A detector, which measures the energy of a e^{\pm} or a high energy γ by fully absorbing it \rightarrow destructive method!

Longitudinal profile $\frac{dE}{dt} \propto t^\alpha e^{-t}$

Shower maximum at $t_{\max} = \ln \frac{E_0}{E_c} \frac{1}{\ln 2}$

95% containment $t_{95\%} \approx t_{\max} + 0.08Z + 9.6$

Size of a calorimeter grows only logarithmically with E_0

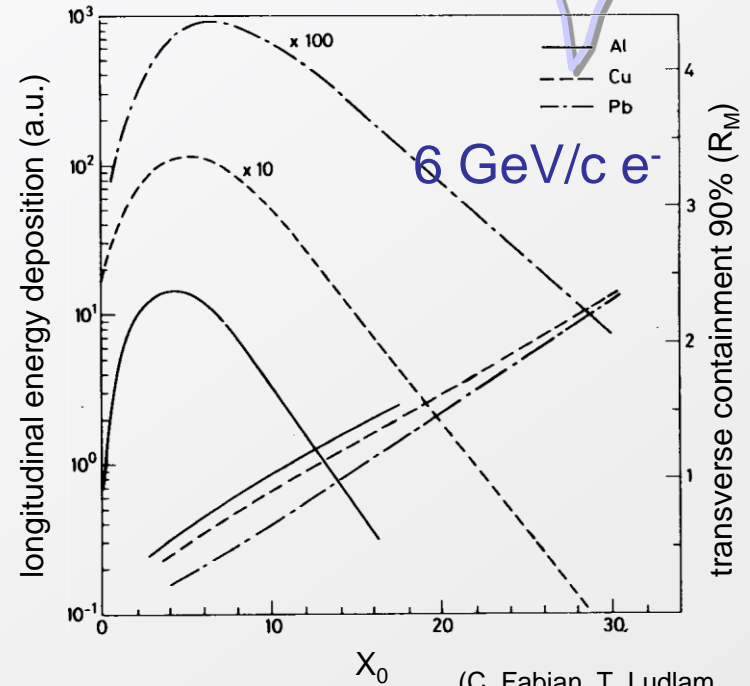
- Transverse shower development: 95% of the shower cone is located in a cylinder with radius $2 R_M$

$$R_M = \frac{21 \text{ MeV}}{E_c} X_0 \quad [g/cm^2] \quad \text{Molière radius}$$

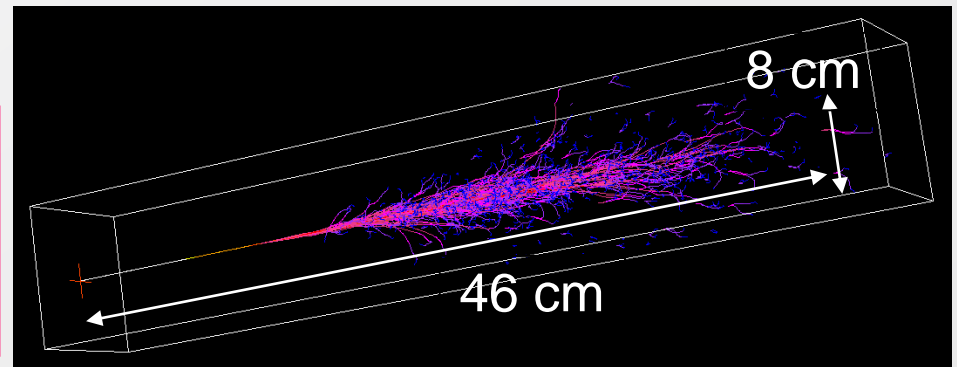
Example: $E_0 = 100 \text{ GeV}$ in lead glass

$E_c = 11.8 \text{ MeV} \rightarrow t_{\max} \approx 13, t_{95\%} \approx 23$

$X_0 \approx 2 \text{ cm}, R_M = 1.8 \cdot X_0 \approx 3.6 \text{ cm}$



(C. Fabjan, T. Ludlam, CERN-EP/82-37)



General expression

$$\frac{\sigma(E)}{E} = \frac{a}{\sqrt{E}} \oplus b \oplus \frac{c}{E}$$

Also true for hadronic showers (see below)

Also spatial and angular resolution scale like $1/\sqrt{E}$

stochastic term

'constant term'

- inhomogenities
- bad cell inter-calibration
- non-linearities

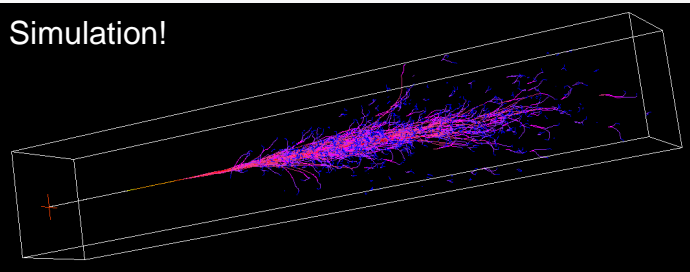
Quality factor !

'noise term'

- Electronic noise
- radioactivity
- pile up

Homogeneous calorimeter

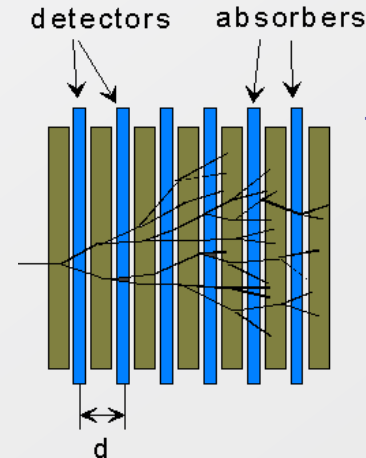
Absorber = active material.



High E-resolution, no longitudinal shower information. High cost.

Sampling calorimeter

Absorber and active detector layers.

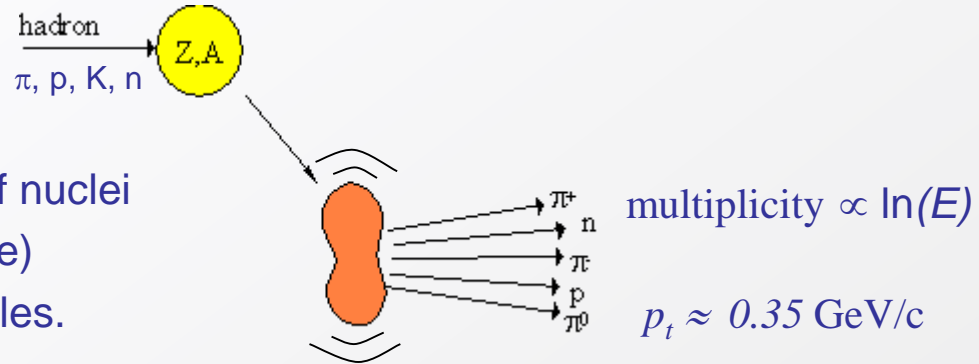


Extra sampling fluctuations

$$\frac{\sigma(E)}{E} \propto \sqrt{\frac{d}{E}}$$

Shower 'image'
Lower cost.

The interaction of energetic hadrons (charged or neutral) with matter is dominated by **inelastic nuclear processes**.



Excitation and finally break-up of nuclei
 → nuclear fragments (radioactive)
 + production of secondary particles.

For high energies ($>1 \text{ GeV}$) the cross-sections depend only little on the energy and on the type of the incident particle (π, p, K, \dots).

$$\sigma_{inel} \approx \sigma_0 A^{0.7} \quad \sigma_0 \approx 35 \text{ mb}$$

In analogy to X_0 a hadronic absorption length can be defined

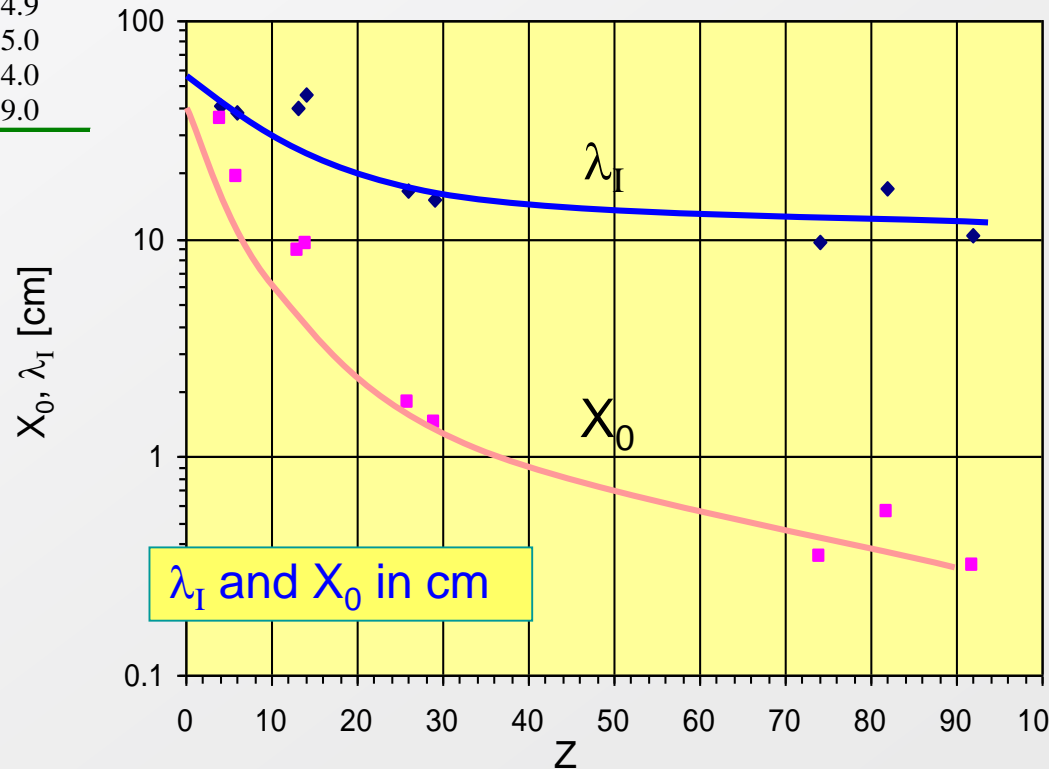
$$\lambda_a = \frac{A}{N_A \sigma_{inel}} \propto A^{\frac{1}{4}} \quad \text{because } \sigma_{inel} \approx \sigma_0 A^{0.7}$$

similarly a hadronic interaction length

$$\lambda_I = \frac{A}{N_A \sigma_{total}} \propto A^{\frac{1}{3}} \quad \lambda_I < \lambda_a$$

Material	Z	A	ρ [g/cm ³]	X_0 [g/cm ²]	λ_I [g/cm ²]
Hydrogen (gas)	1	1.01	0.0899 (g/l)	63	50.8
Helium (gas)	2	4.00	0.1786 (g/l)	94	65.1
Beryllium	4	9.01	1.848	65.19	75.2
Carbon	6	12.01	2.265	43	86.3
Nitrogen (gas)	7	14.01	1.25 (g/l)	38	87.8
Oxygen (gas)	8	16.00	1.428 (g/l)	34	91.0
Aluminium	13	26.98	2.7	24	106.4
Silicon	14	28.09	2.33	22	106.0
Iron	26	55.85	7.87	13.9	131.9
Copper	29	63.55	8.96	12.9	134.9
Tungsten	74	183.85	19.3	6.8	185.0
Lead	82	207.19	11.35	6.4	194.0
Uranium	92	238.03	18.95	6.0	199.0

For $Z > 6$: $\lambda_I > X_0$

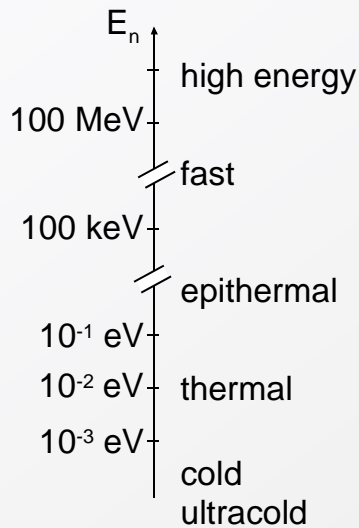
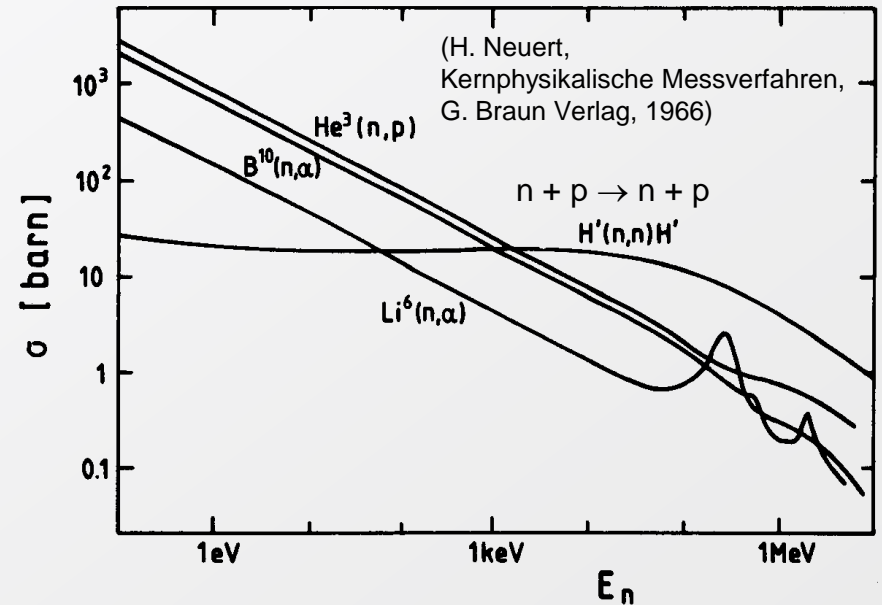
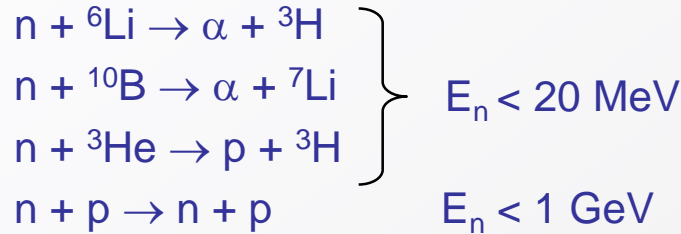


Interaction of neutrons and neutrinos

Interaction of neutrons

Neutrons have no charge, i.e. their interaction is based only on strong (and weak) nuclear force. To detect neutrons, we have to create charged particles.

Use neutron conversion and elastic reactions ...

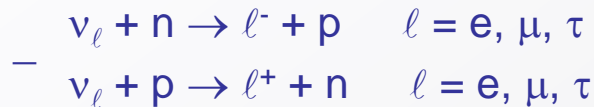


In addition there are ...

- neutron induced fission $E_n \approx E_{th} \approx 1/40 \text{ eV}$
- inelastic reactions $E_n > 1 \text{ GeV}$

■ Interaction of neutrinos

Neutrinos interact only weakly → tiny cross-sections. For their detection we need again first a charged particle. Possible detection reactions:



The cross-section for the reaction $\nu_e + n \rightarrow e^- + p$ is of the order of 10^{-43} cm^2 (per nucleon, $E_\nu \approx \text{few MeV}$).

→ detection efficiency $\varepsilon_{\text{det}} = \sigma \cdot N_a = \sigma \cdot \rho \frac{N_A}{A} d$ (N_a : area density $\neq N_A$: Avogadro's number)

1 m Iron: $\varepsilon_{\text{det}} \approx 5 \cdot 10^{-17}$

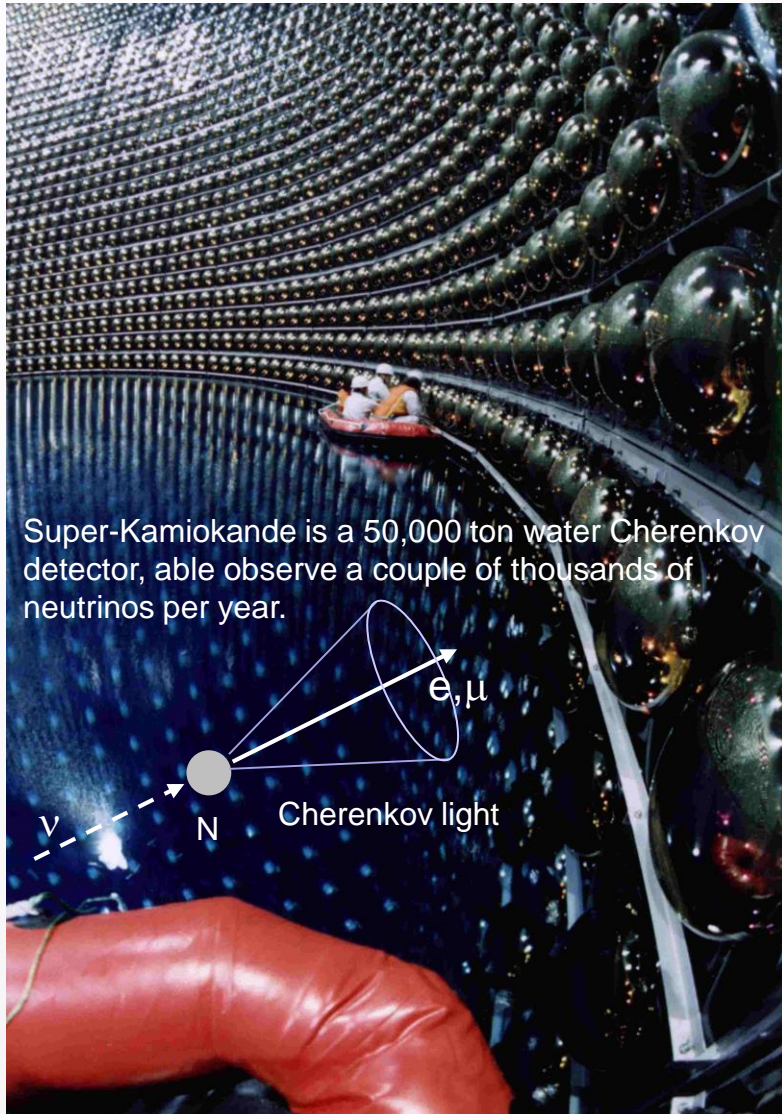
1 km water: $\varepsilon_{\text{det}} \approx 6 \cdot 10^{-15}$

Neutrino detection requires big and massive detectors (ktons - Mtons) and very high neutrino fluxes (e.g. $10^{20} \nu / \text{yr}$).

In collider experiments fully **hermetic** detectors allow to detect neutrinos indirectly:

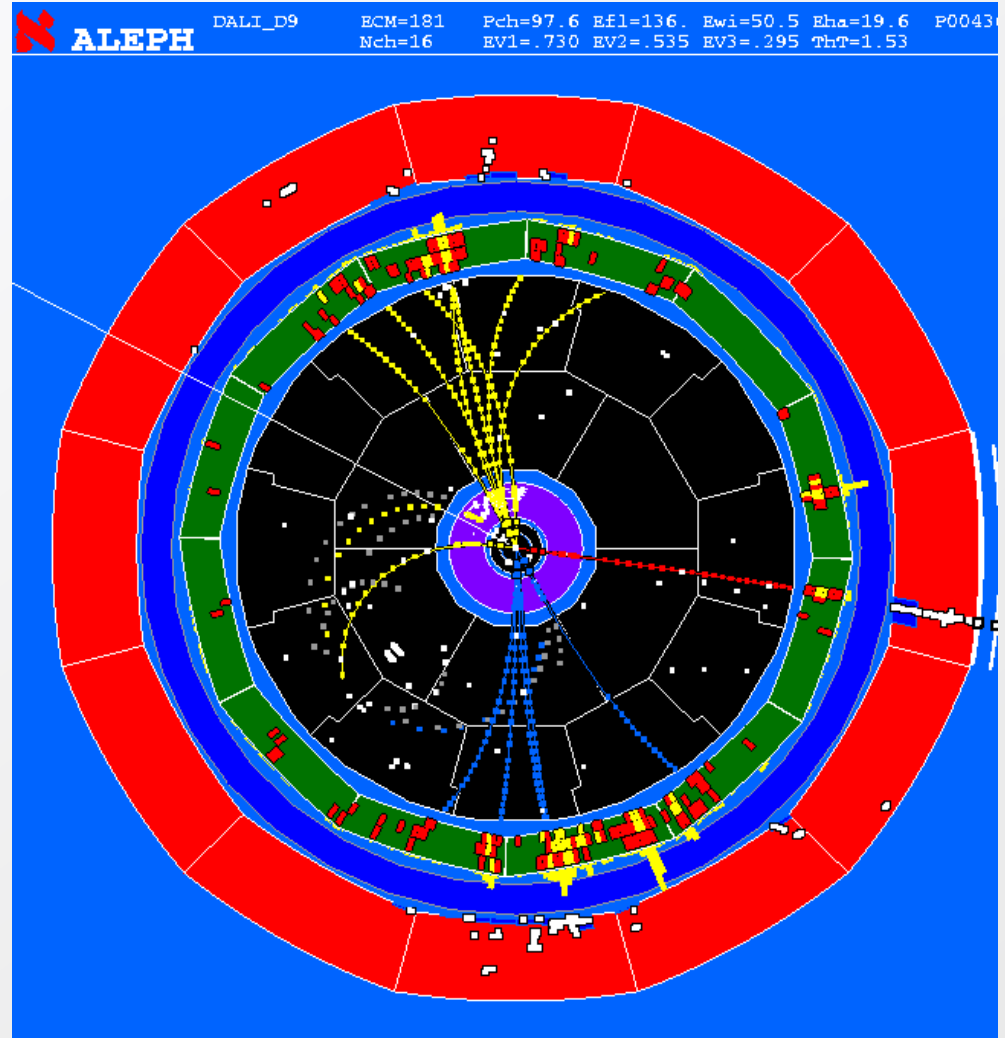
- sum up all visible energy and momentum.
- attribute missing energy and momentum to neutrino.

Direct neutrino detection



Indirect neutrino detection

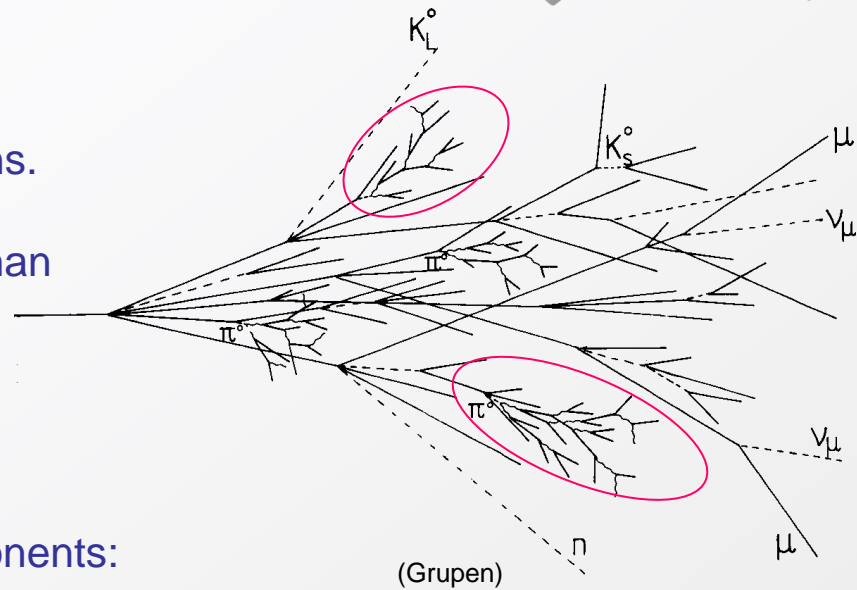
$e^+e^- (\sqrt{s}=181 \text{ GeV}) \rightarrow W^+W^- \rightarrow qq\mu\nu_\mu$
 $\rightarrow 2 \text{ hadronic jets} + \mu + \text{missing momentum}$



Hadronic cascades

Lots of processes involved:
Strong, e.m. and weak interactions.

Much more complex and larger than
electromagnetic cascades.
($\lambda_1 > X_0$)



A hadronic shower has two components:

hadronic

+

electromagnetic



- charged hadrons p, π^\pm, K^\pm ,
- nuclear fragments
- breaking up of nuclei (binding energy)
- neutrons, neutrinos, soft γ 's, muons



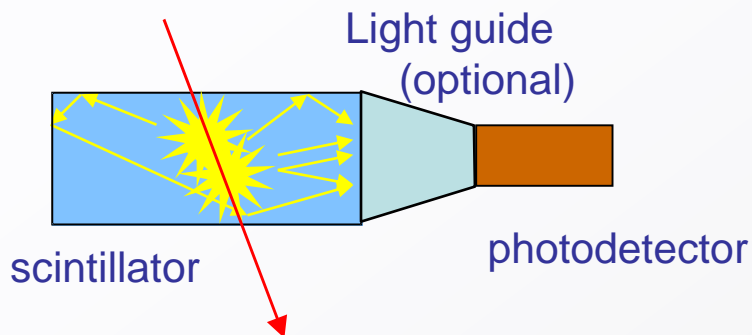
neutral pions $\pi^0 \rightarrow 2\gamma$

→ electromagnetic cascades

$$n(\pi^0) \approx \ln E(\text{GeV}) - 4.6$$

example $E = 100 \text{ GeV}$: $n(\pi^0) \approx 18$

invisible energy → large fluctuations of visible energy
→ Modest energy resolution of hadronic calorimeters.



Energy deposition by an ionizing particle or photon (γ)

- generation
- transmission
- detection



Two categories

Organic scintillators
(crystals, plastics or liquid solutions)

- Up to 10000 photons per MeV
- Low Z (not good for photoeffect)
- Low density $\rho \sim 1\text{g/cm}^3$
- Doped, large choice of emission wavelength
- ns decay times
- Relatively inexpensive
- Medium Rad. Hard (10 kGy/year)
- Used in hadr./e.m. calorimetry, as trigger counters, for lab tests



Inorganic
(crystalline structure)

- More light (up to 70000 ph/MeV)
- High Z, high density
- Rel. expensive
- Used in e.m. calorimetry

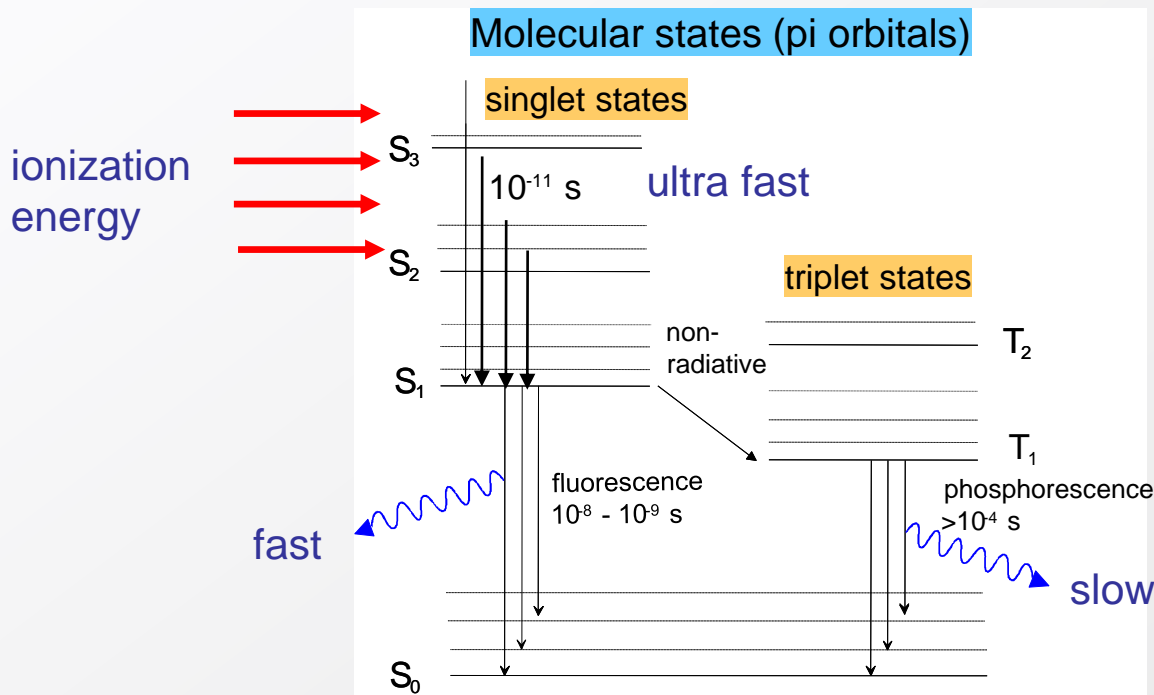
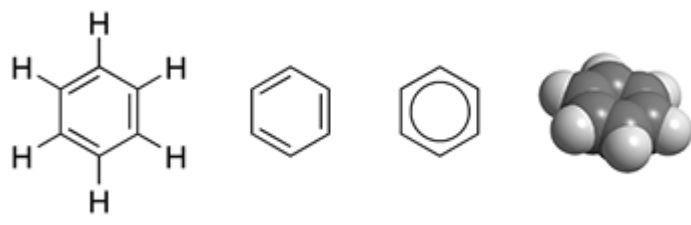
Don't confuse scintillators with **lead glass** !



The light generation in lead glass is actually based on the Cherenkov effect. Lead glass is the poor man's crystal. High density, but little light output.

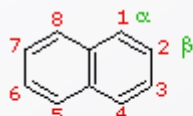
Organic scintillation mechanism

The organic scintillation mechanism is based on the pi-electrons (molecular orbitals) of the benzene ring (C_6H_6).

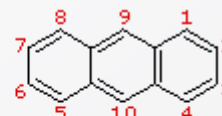


Organic scintillators exist as

crystals
(very rarely used in HEP)

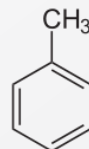


naphthalene
 $C_{10}H_8$
m.p. 81° C

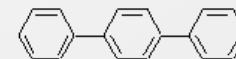


anthracene
 $C_{14}H_{10}$
m.p. 217° C

liquids
(solutions)
(rarely used in HEP)



e.g. toluene



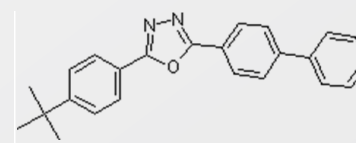
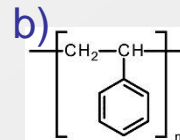
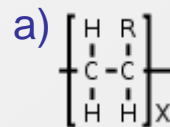
e.g. p-terphenyl

solvent

+

activator

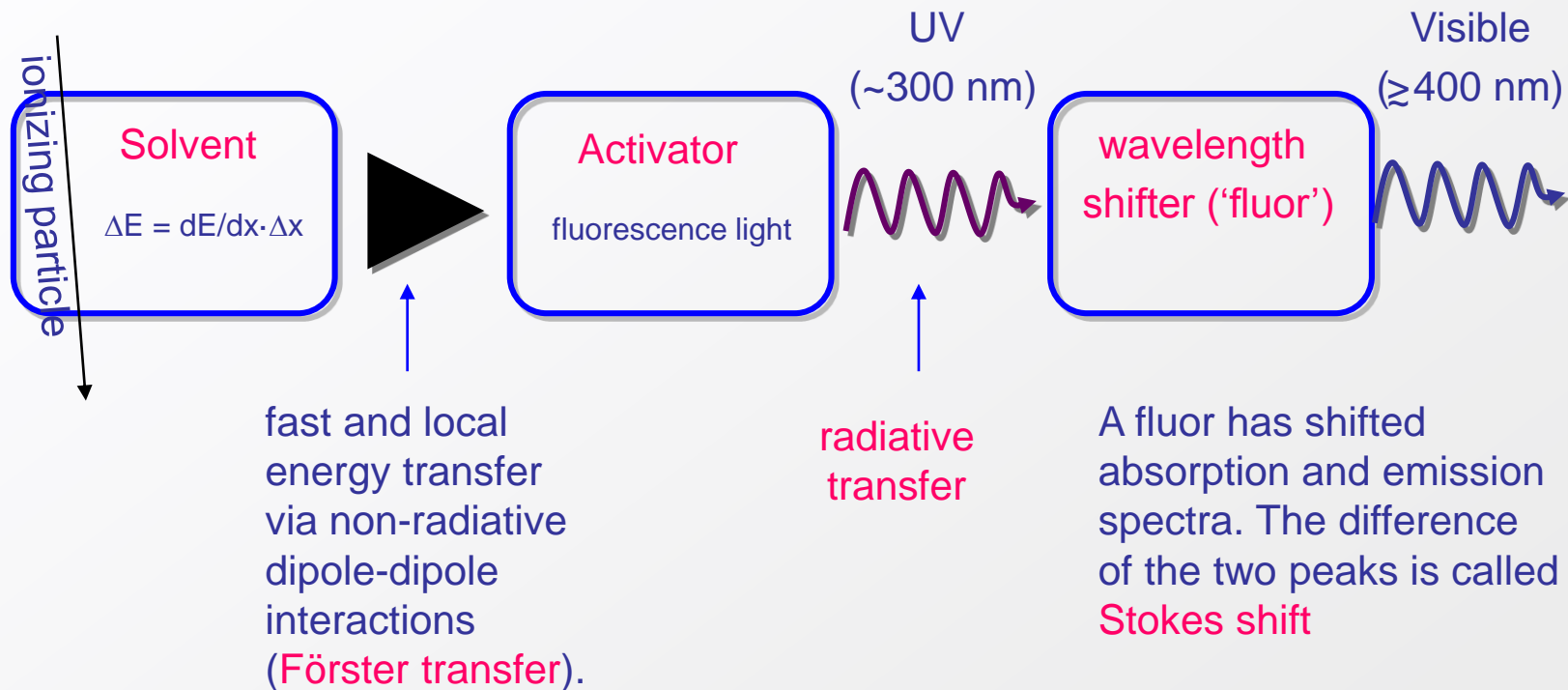
plastics
(polymerized solutions)
(much used in HEP)



e.g. Butyl-PBD

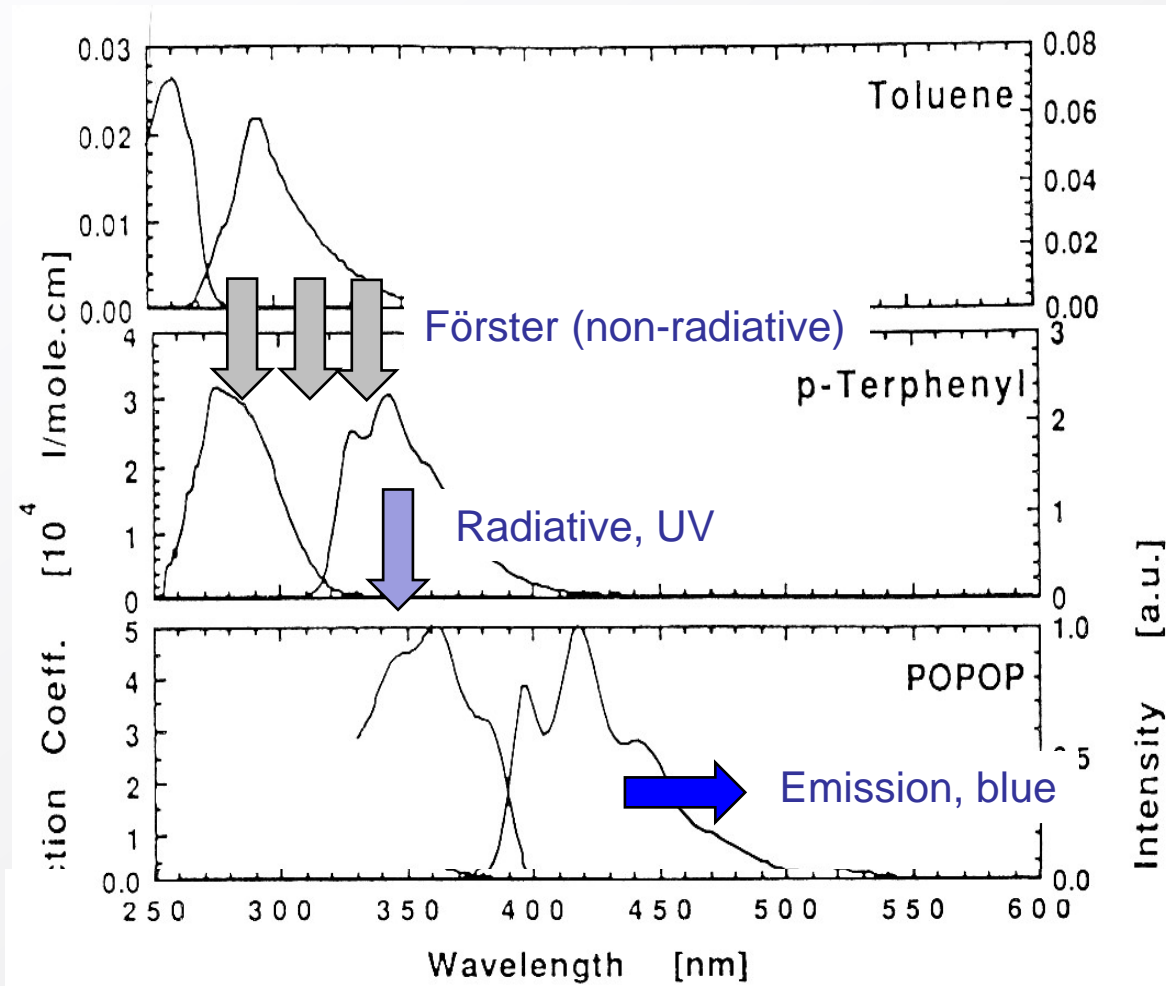
e.g. polyvinyltoluene (a) or polystyrene (b)

Often they consist of a **solvent + activator** and a secondary fluor as **wavelength shifter**.



Two dopant scheme for plastic scintillators

Abs. and emission spectra



Some examples of commercial plastic scintillators. There are just two main suppliers: (Saint Gobain, FR/US) or ELJEN (US) which deliver rather comparable products.

Physical Constants of SGC Plastic Scintillators

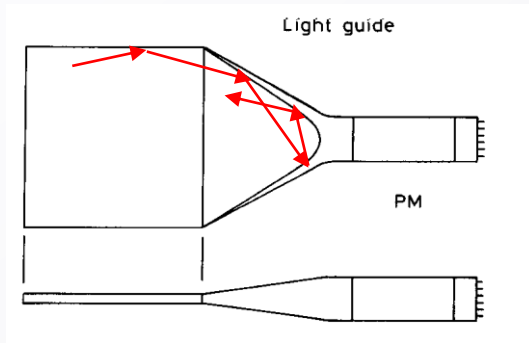
Scintillator	Light Output % Anthracene ¹	Wavelength of Maximum Emission, nm	Decay Constant, Main Component, ns	Bulk Light Attenuation Length, cm	Refractive Index	H:C Ratio	Loading Element % by weight	Density	Softening Point °C
BC-400	65	423	2.4	250	1.58	1.103		1.032	70
BC-404	68	408	1.8	160	1.58	1.107		1.032	70
BC-408	64	425	2.1	380	1.58	1.104		1.032	70
BC-412	60	434	3.3	400	1.58	1.104		1.032	70
BC-414	68	392	1.8	100	1.58	1.110		1.032	70
BC-416	38	434	4.0	400	1.58	1.110		1.032	70
BC-418	67	391	1.4	100	1.58	1.100		1.032	70
BC-420	64	391	1.5	110	1.58	1.102		1.032	70
BC-422	55	370	1.6	8	1.58	1.102		1.032	70
BC-422Q	11	370	0.7	<8	1.58	1.102	Benzephenone,0.5%*	1.032	70
BC-428	36	480	12.5	150	1.58	1.103		1.032	70
BC-430	45	580	16.8	NA	1.58	1.108		1.032	70

≈8000 photons / MeV

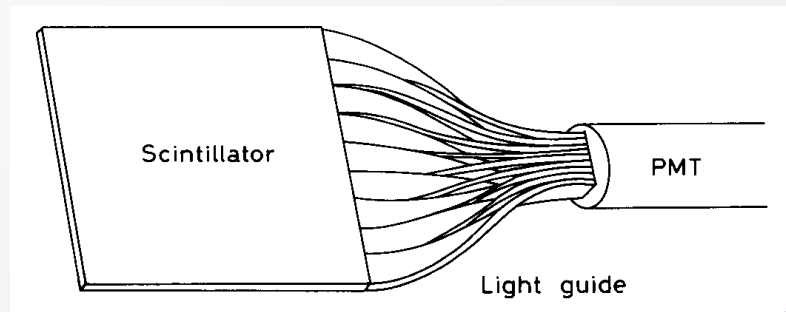
Readout has to be adapted to geometry, granularity and emission spectrum of scintillator.

Geometrical adaptation:

- **Light guides:** transfer by total internal reflection (+outer reflector)

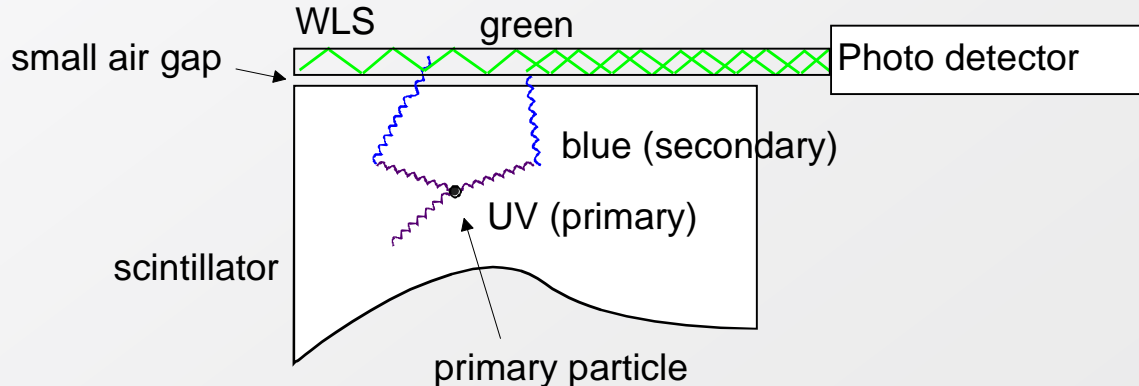


“fish tail”



adiabatic

- **Wavelength shifter (WLS) bars / fibres**



Watch out: it's very hard to beat Liouville!

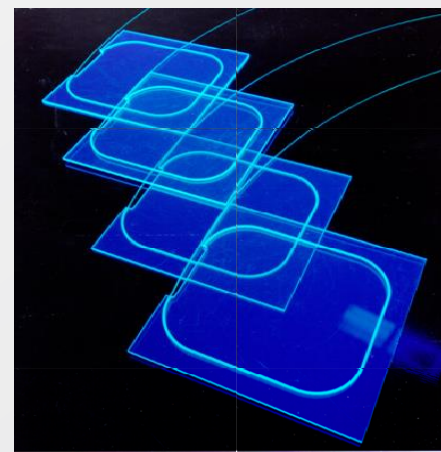
- Large volume liquid or solid detectors
- neutron detection
- underground experiments
- sampling calorimeters (**HCAL** in **CMS** or **ATLAS**, etc.),
- trigger counters,
- TOF counters,
- Fibre tracking
(see below)



Plastic scintillators in various shapes (Saint Gobain)

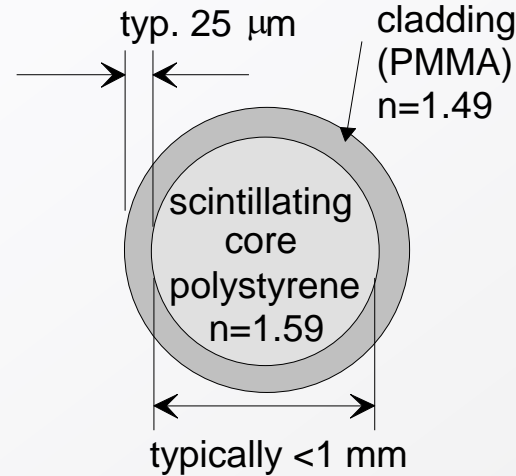
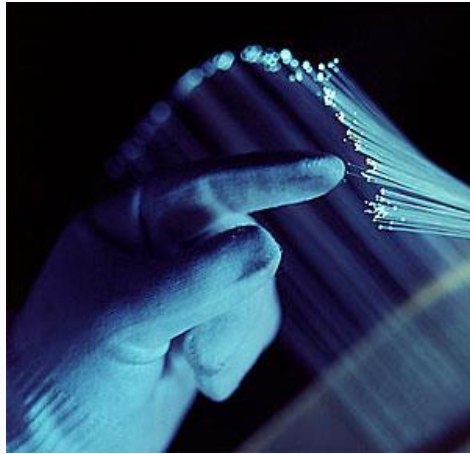


Michigan University: 'neutron wall'. The flat-sided glass tubes contain liquid scintillator.

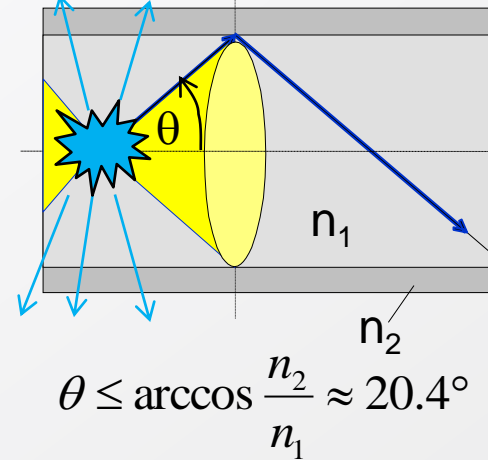


Scintillating tiles of CMS HCAL.

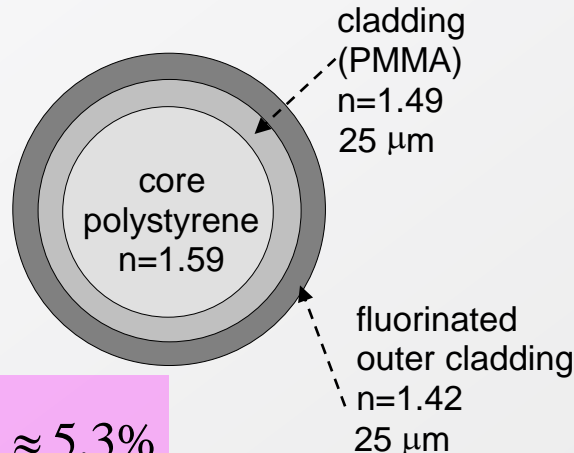
Working principle of scintillating plastic fibres :



light transport by total internal reflection



Double cladding system (developed by CERN RD7)



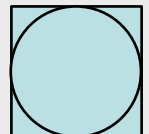
$$\frac{d\Omega}{4\pi} = 0.5 (1 - \cos \theta) \approx 5.3\%$$

Trapping fraction

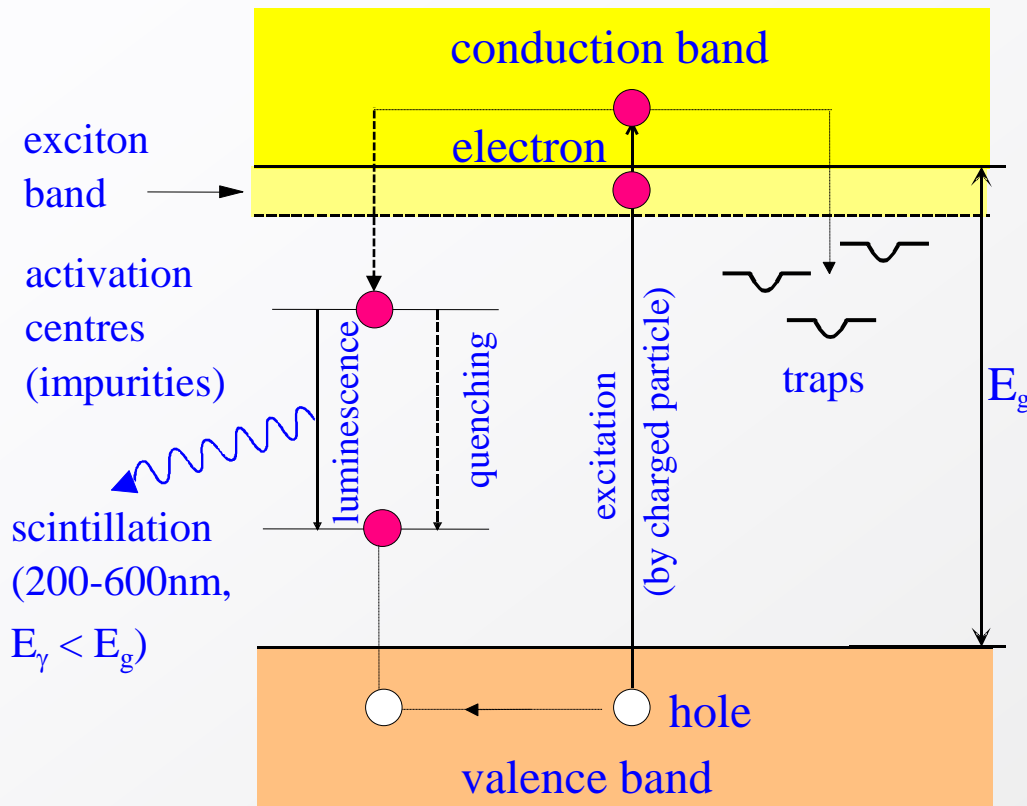
$$\frac{d\Omega}{4\pi} = 0.5 (1 - \cos \theta) \approx 3\%$$

(per side)

There are also square fibres. Their trapping fraction is slightly higher (additional angular phase space), but corners are problematic for light transport.



- Based on band structure of a crystal. Does not work for liquids or gases.

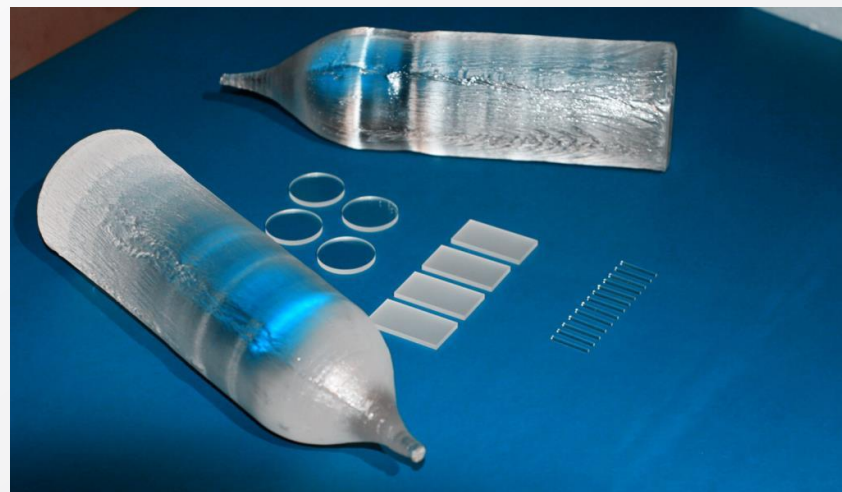
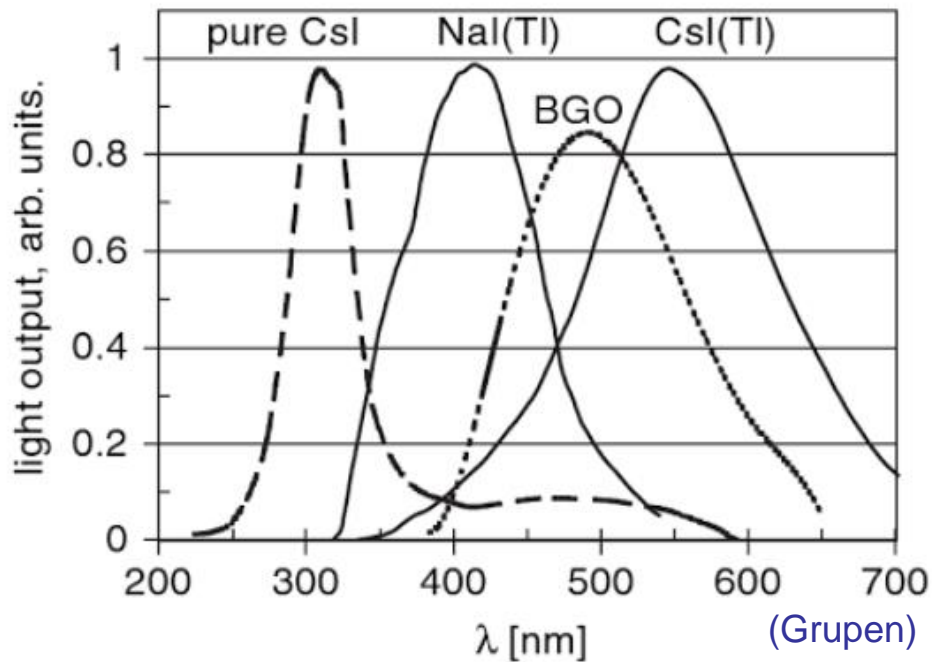


Exception: Liquefied noble gases scintillate, too. Different process. Not treated here.

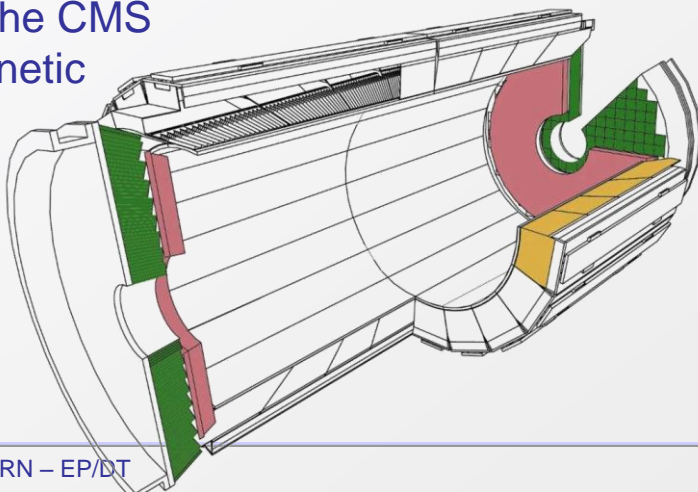
Band gap E_g should be large (>3 eV) to ensure that crystal is transparent.

Warning: sometimes ≥ 2 time constants:

- fast recombination (ns- μ s) from activation centers
- delayed recombination due to trapping (μ s-ms)



~75000 PbWO_4 crystals in the CMS electromagnetic calorimeter





Please wake up

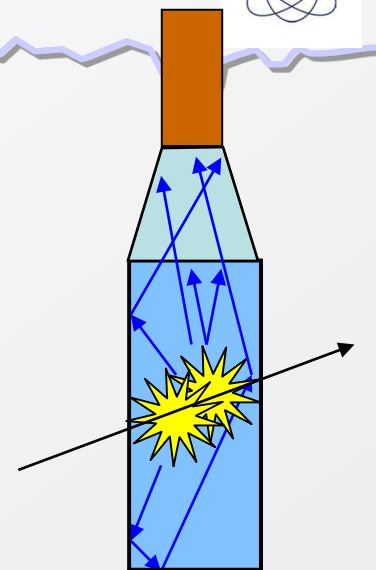
New topic: Photodetection

(Detection of light in the optical domain)

The classical domains of application

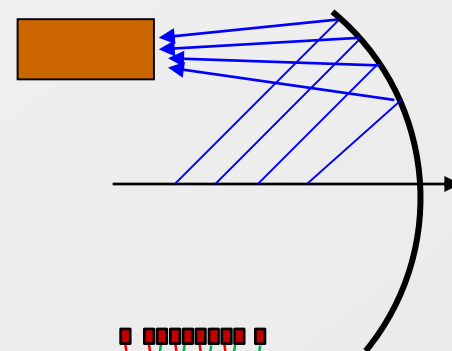
☐ Calorimetry

- Readout of organic and inorganic scintillators, lead glass, scint. or quartz fibres → Blue/VIS, usually 10s – 10000s of photons



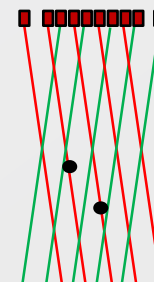
☐ Particle Identification

- Detection of Cherenkov light → UV/blue, single photons
- Time Of Flight → Usually readout of organic scintillators (not competitive at high momenta) or Cherenkov radiators



☐ Tracking

- Readout of scintillating fibres → blue/VIS, few photons



Basics of photon detection

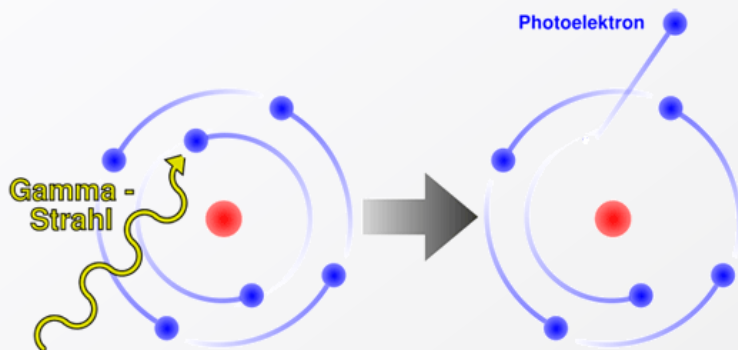
Purpose:

Convert light into detectable electronic signal

(we are not covering photographic emulsions!)

Principle:

Use photoelectric effect to 'convert' photons (γ) to photoelectrons (pe)

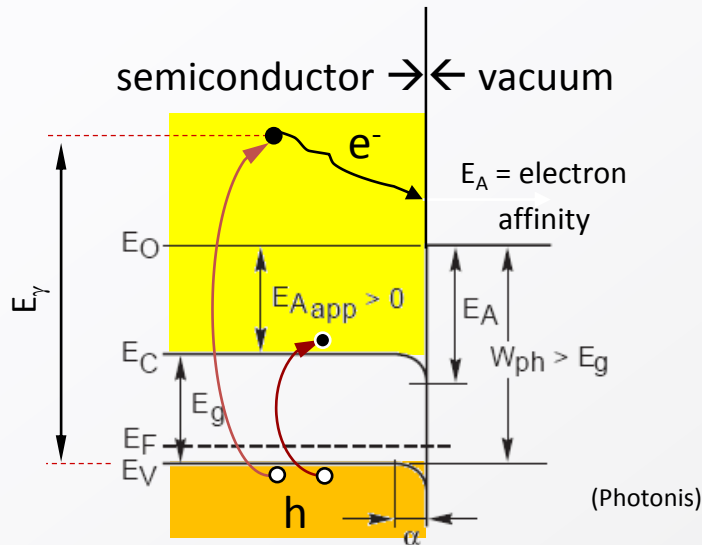


Details depend on the type of the photosensitive material (see below).

Photon detection involves often materials like K, Na, Rb, Cs (alkali metals) . They have the smallest electronegativity \rightarrow highest tendency to release electrons.

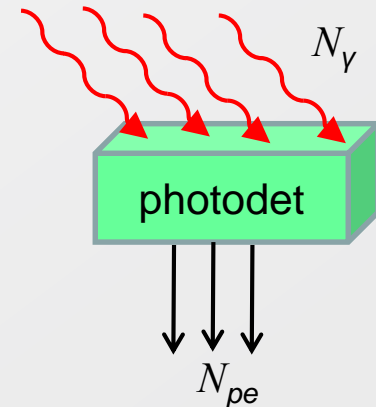
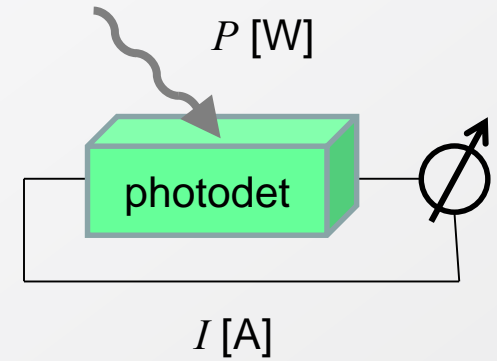
Basics of photodetection

Many photosensitive materials are semiconductors, but photoeffect can also be observed from gases and liquids.



Internal photoeffect

External photoeffect



Internal photoeffect: $E_\gamma > E_g$

External photoeffect: $E_\gamma > E_g + E_A$

Requirements on photodetectors

- High **sensitivity**, usually expressed as: quantum efficiency $QE(\%) = \frac{N_{pe}}{N_\gamma}$

or radiant sensitivity S (mA/W), with $QE(\%) \approx 124 \cdot \frac{S(mA/W)}{\lambda(nm)}$

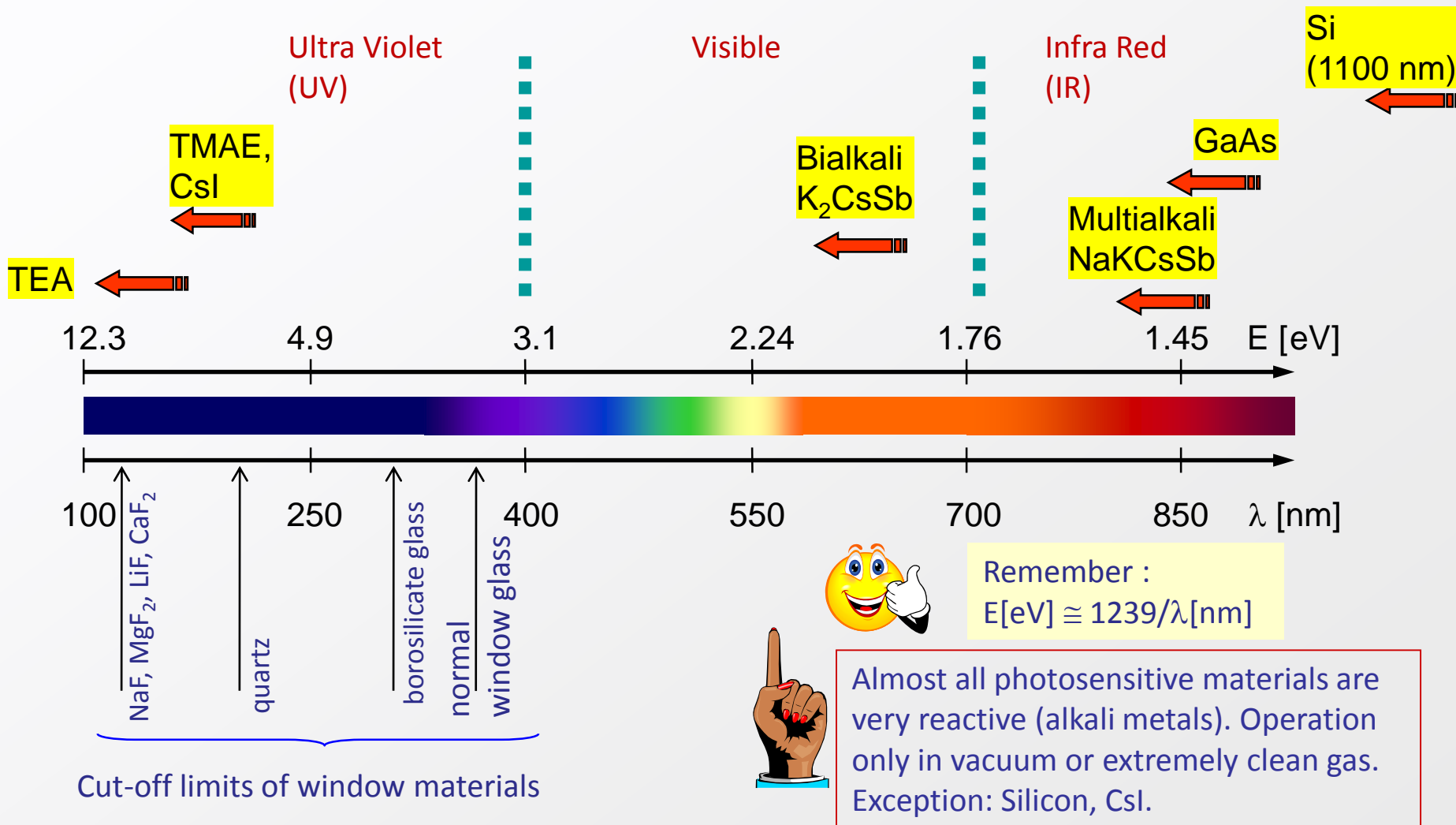


QE can be >100% (for high energetic photons) !

- Good **Linearity**: Output signal \sim light intensity, over a large dynamic range (critical e.g. in calorimetry (energy measurement)).
- Fast **Time response**: Signal is produced instantaneously (within ns), low jitter (<ns), no afterpulses
- **Low intrinsic noise**. A noise-free detector doesn't exist. Thermally created photoelectrons represent the lower limit for the noise rate $\sim A_0 T^2 \exp(-eW_{ph}/kT)$. In many detector types, noise is dominated by other sources.
- + many more (size, fill factor, radiation hardness, cost, tolerance/immunity to B-fields...)

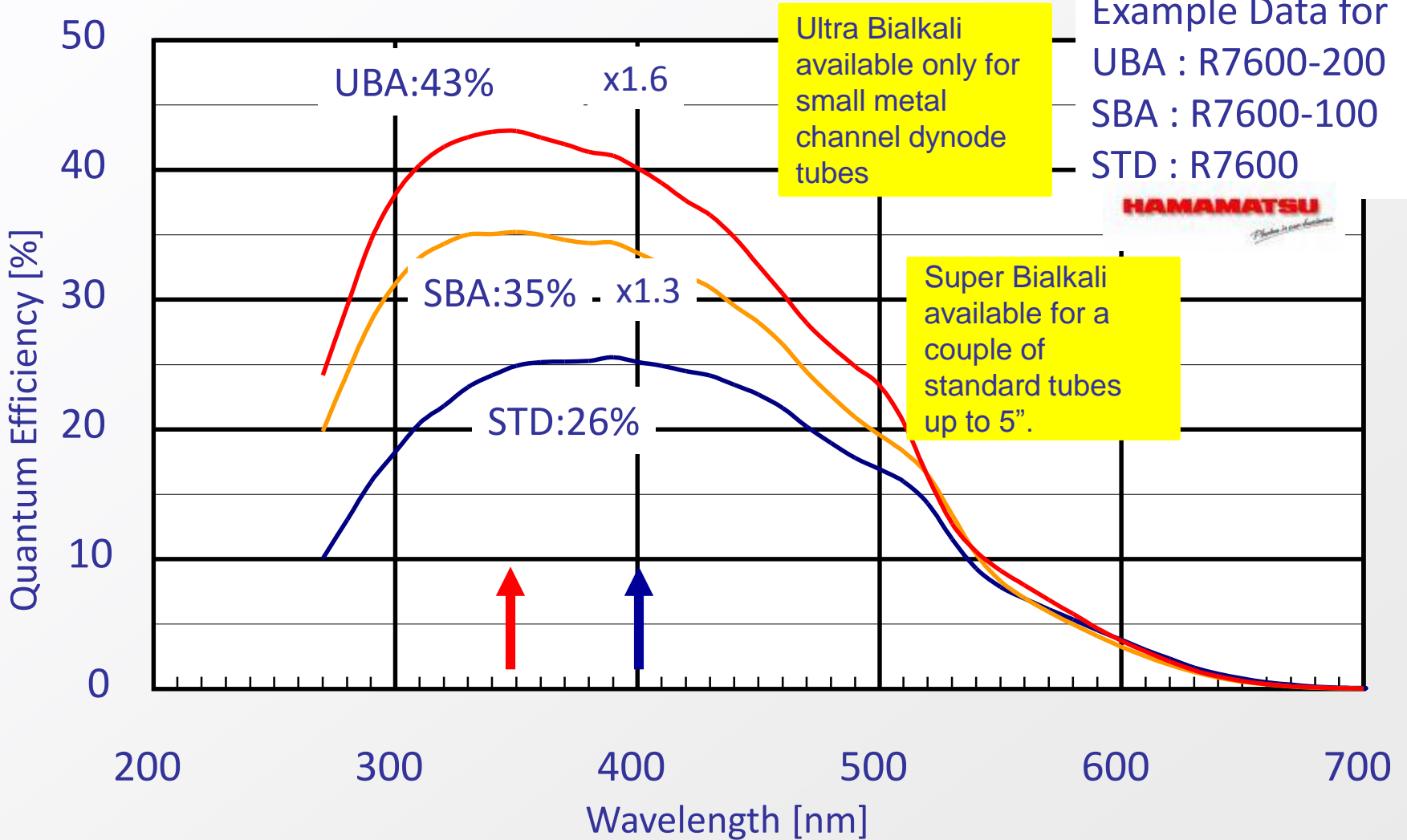
Frequently used photosensitive materials / photocathodes

← begin of arrow indicates threshold



Latest generation of high performance photocathodes

QE Comparison of semitransparent bialkali QE



Basic principle:

Photo-emission from photo-cathode

Secondary emission from N dynodes:

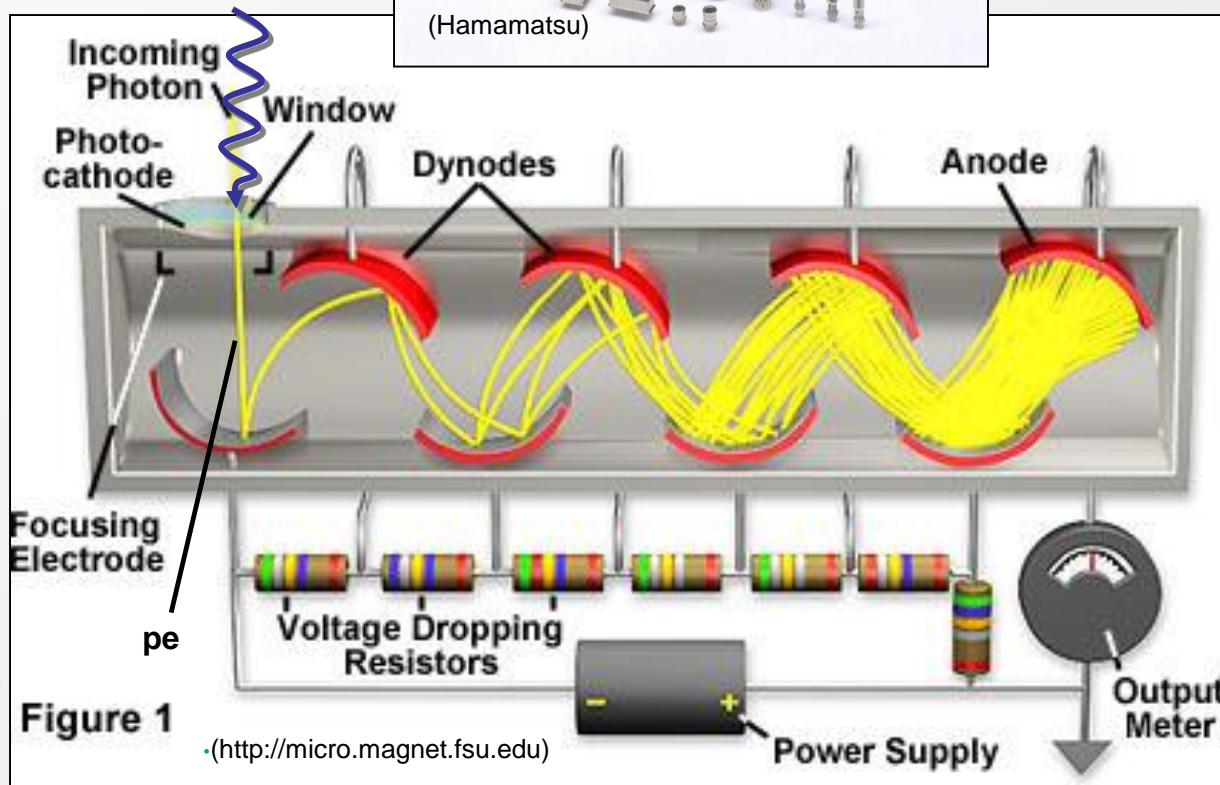
- dynode gain $g \approx 3-50$ (function of incoming electron energy E);
- total gain M :

$$M = \prod_{i=1}^N g_i$$

Example:

- 10 dynodes with $g = 4$
- $M = 4^{10} \approx 10^6$

Very sensitive to magnetic fields, even to earth magnetic field ($30-60 \mu\text{T} = 0.3-0.6$ Gauss).
 → Shielding required (mu-metal).



- Mainly determined by the fluctuations of the number of secondary electrons m_i emitted from the dynodes;

- Poisson distribution:

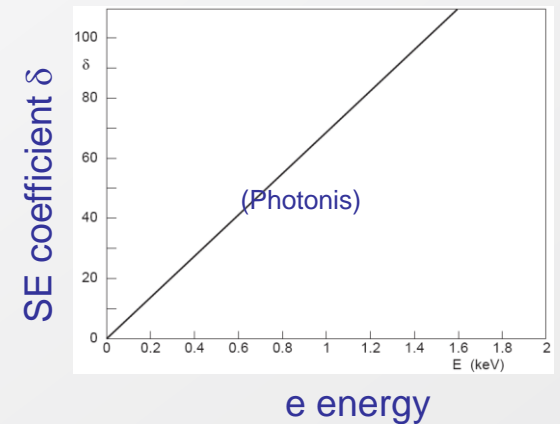
$$P(n, m_i) = \frac{m_i^n e^{-m_i}}{n!}$$

- Standard deviation:

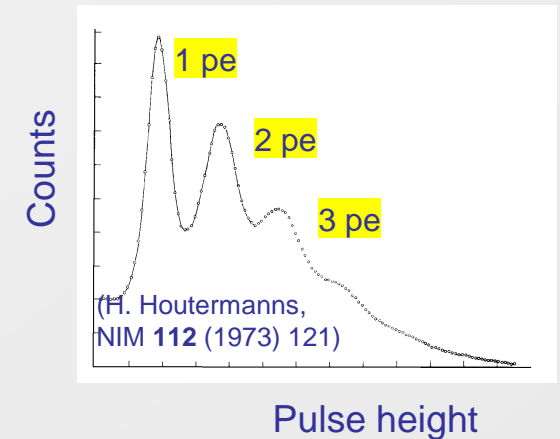
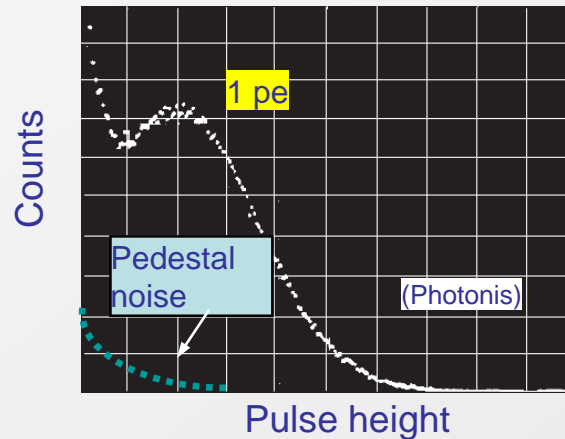
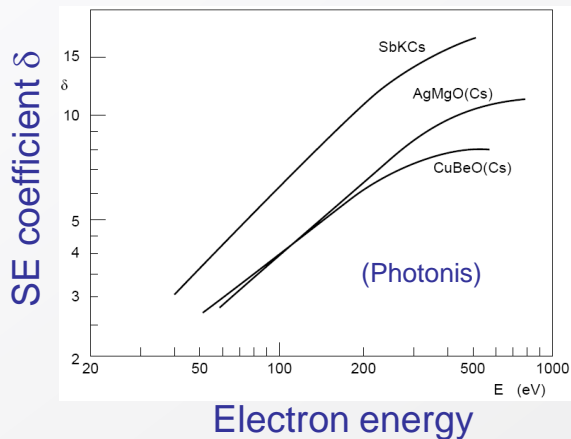
$$\frac{\sigma_n}{m_i} = \frac{\sqrt{m_i}}{m_i} = \frac{1}{\sqrt{m_i}}$$

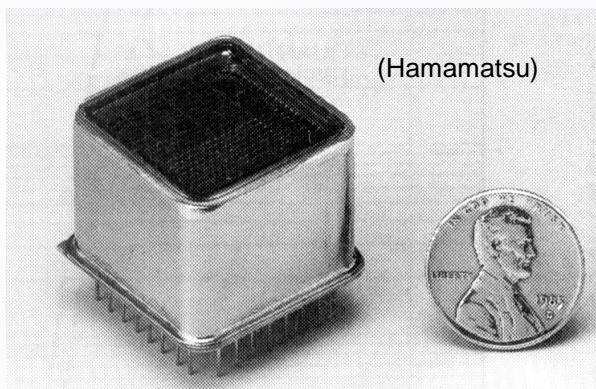
⇒ fluctuations dominated by 1st dynode gain $m_1 = \delta_1$

GaP(Cs) dynodes $E_A < 0$



CuBe dynodes $E_A > 0$

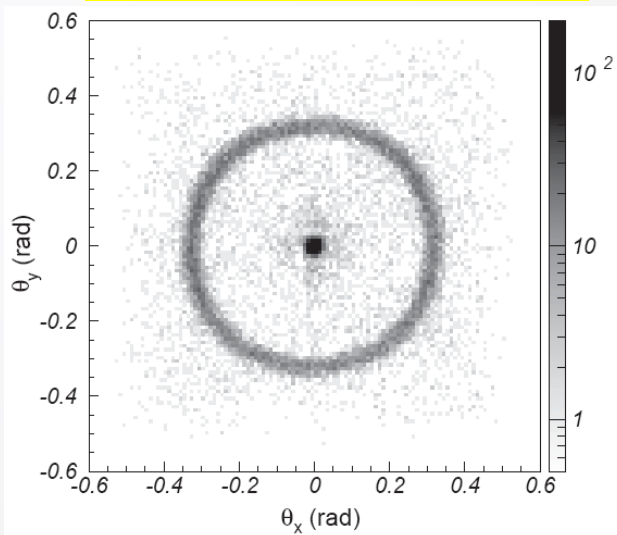




Multi-anode PMT (Hamamatsu)

- Up to 8×8 channels ($2 \times 2 \text{ mm}^2$ each);
- Size: $28 \times 28 \text{ mm}^2$;
- Bialkali PC: $\text{QE} \approx 25 - 45\% @ \lambda_{\text{max}} = 400 \text{ nm}$;
- Gain $\approx 3 \cdot 10^5$;
- Gain uniformity typ. 1 : 2.5;
- Cross-talk typ. 2%

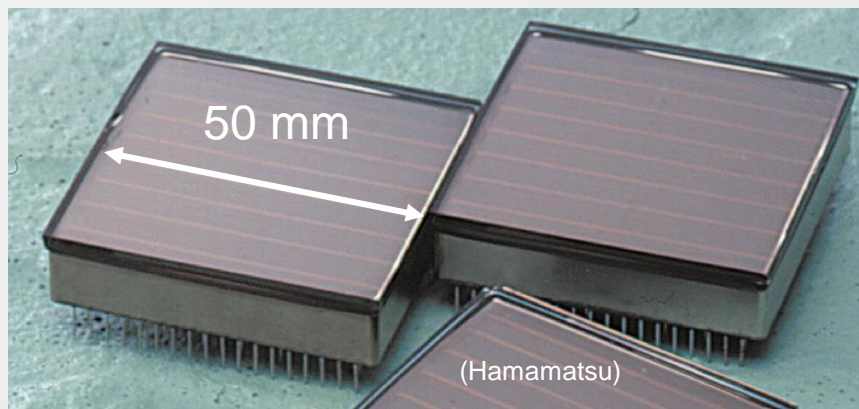
Cherenkov rings from
3 GeV/c π^- through aerogel



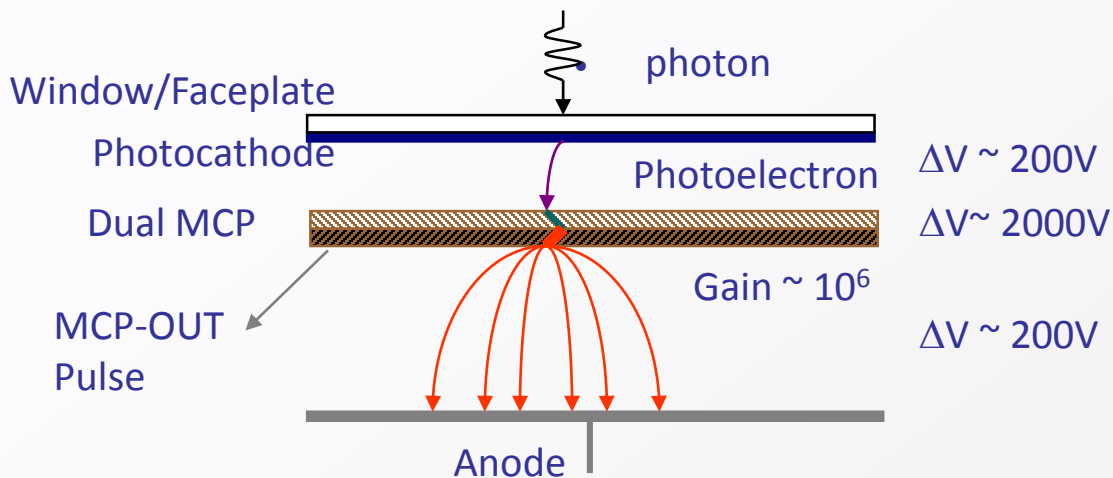
(T. Matsumoto et al., NIMA **521** (2004) 367)

Flat-panel (Hamamatsu H8500):

- 8 x 8 channels ($5.8 \times 5.8 \text{ mm}^2$ each)
- Excellent surface coverage (89%)

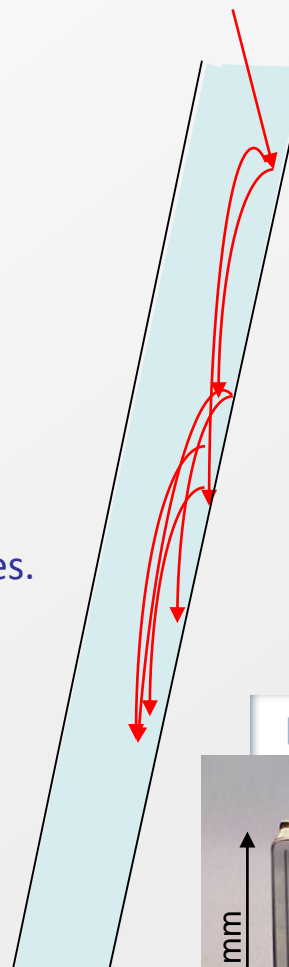
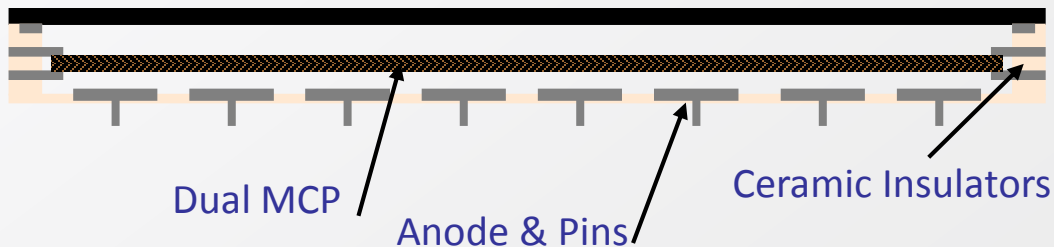


Micro Channel Plate (MCP) based PMTs

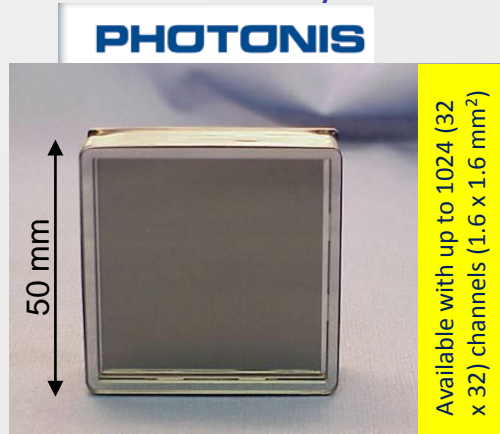


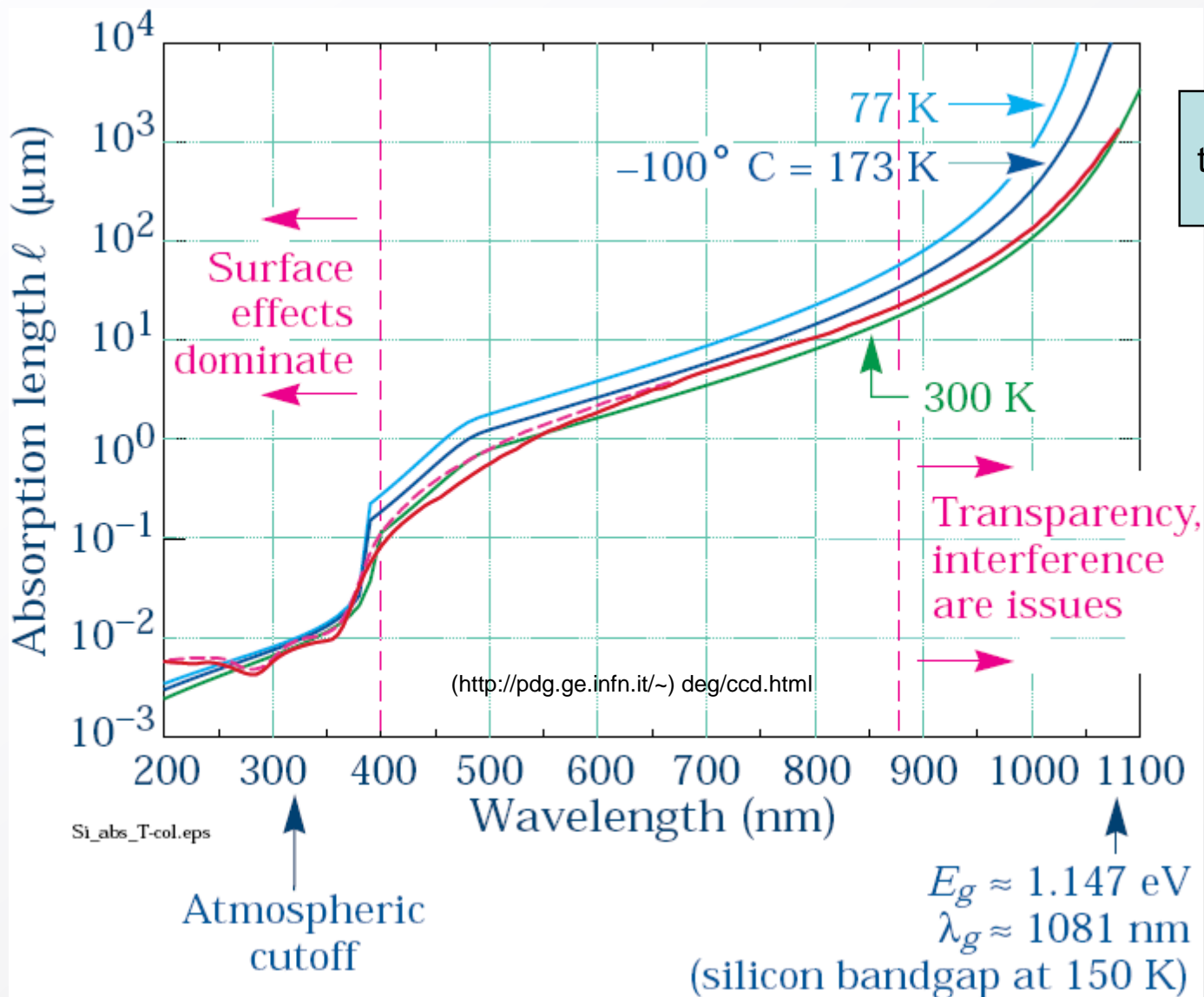
MCPs are usually based on glass disks, with lots of aligned pores. The surface of the pores are metal coated.

Gain stage and detection are decoupled \rightarrow lots of potential and freedom for MA-PMTs: Anode can be easily segmented in application specific way.



- Typical secondary yield is 2
- For 40:1 L:D there are typically 10 strikes ($2^{10} \sim 10^3$ gain per single plate)
- Pore sizes range from <10 to $25 \mu m$.
- Small distances \rightarrow small TTS and good immunity to B-field

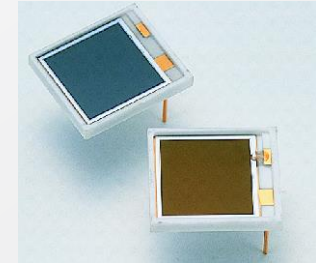
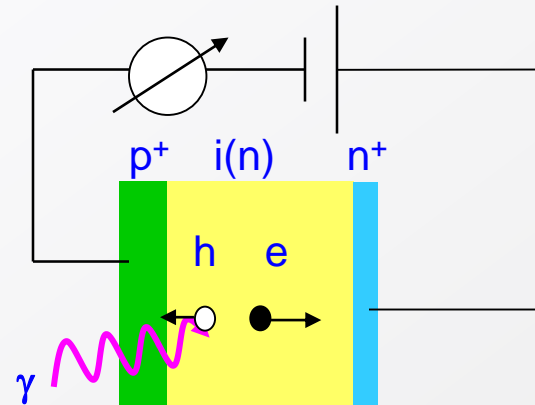




At large λ , temperature effects become important

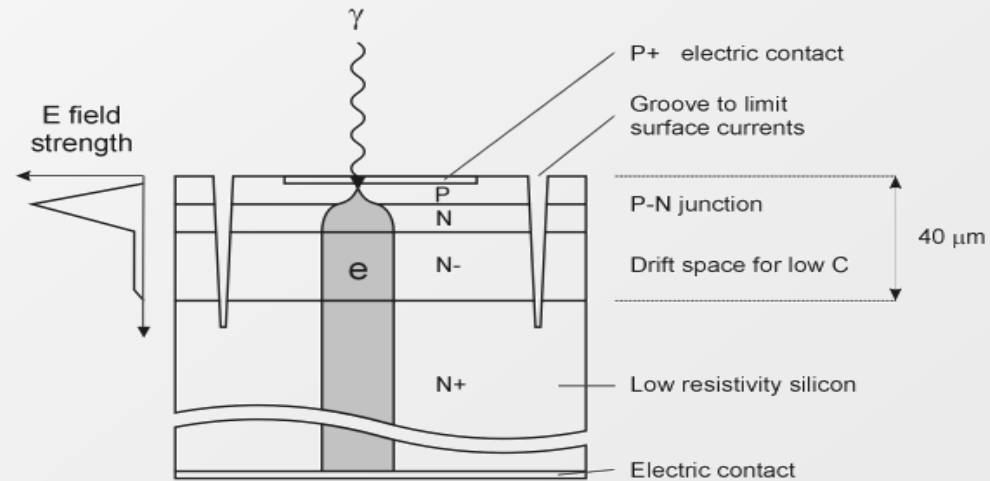
(Si) – Photodiodes (PIN diode)

- P(I)N type
- p layer very thin ($<1 \mu\text{m}$), as visible light is rapidly absorbed by silicon
- High QE (80% @ $\lambda \approx 700\text{nm}$)
- Gain = 1

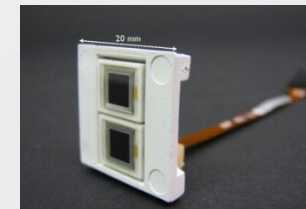


Avalanche photodiode (APD)

- High reverse bias voltage: typ. few 100 V
- Special doping profile \rightarrow high internal field ($>10^5 \text{ V/cm}$) \rightarrow e and h avalanche multiplication
- Avalanche must stop due to statistical fluctuations.
- Gain: typ. $O(100)$
- Rel. high gain fluctuations (excess noise from the avalanche). CMS ECAL APD: $\text{ENF} = 2 @G=50$.
- Very high sensitivity on temp. and bias voltage $\Delta G = 3.1\%/V$ and $-2.4 \%/K$



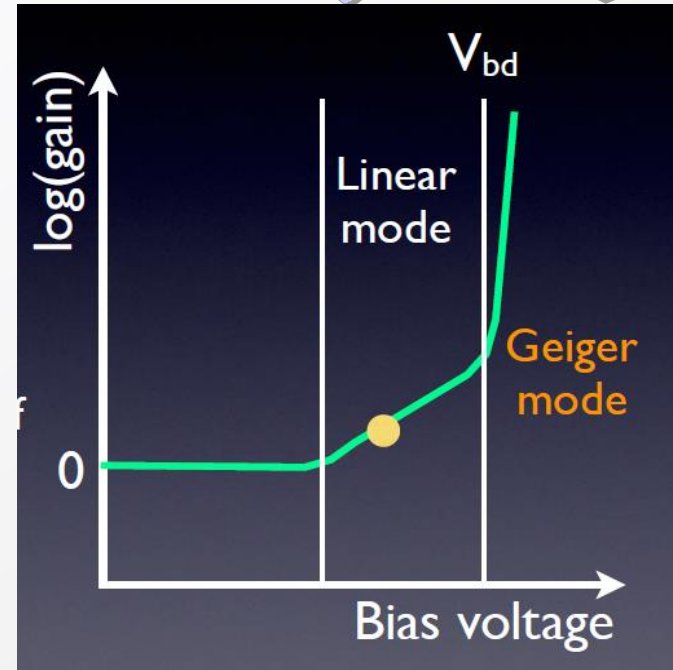
Hamamatsu S8148.
(140.000 pieces used in CMS barrel ECAL).



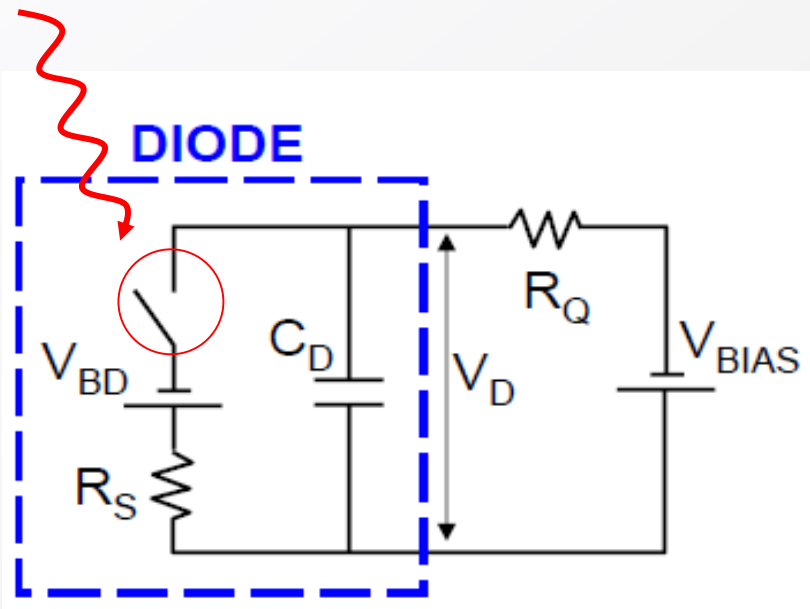
How to obtain higher gain (= single photon detection) without suffering from excessive noise ?

Operate APD cell in Geiger mode (= full discharge), however with (passive) quenching.

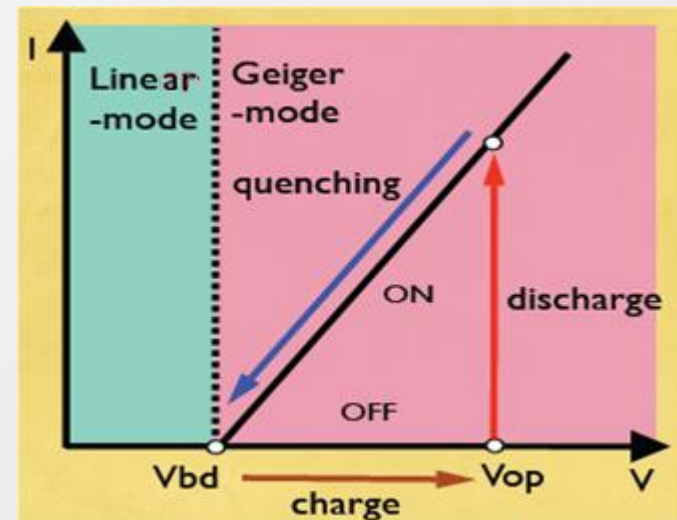
Photon conversion + avalanche short-circuits the diode.



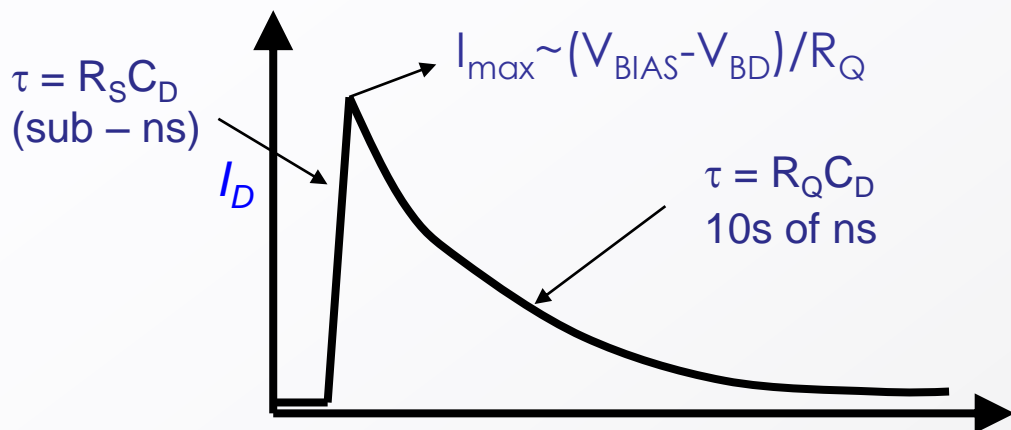
J. Haba, RICH2007



J. Haba, RICH2007

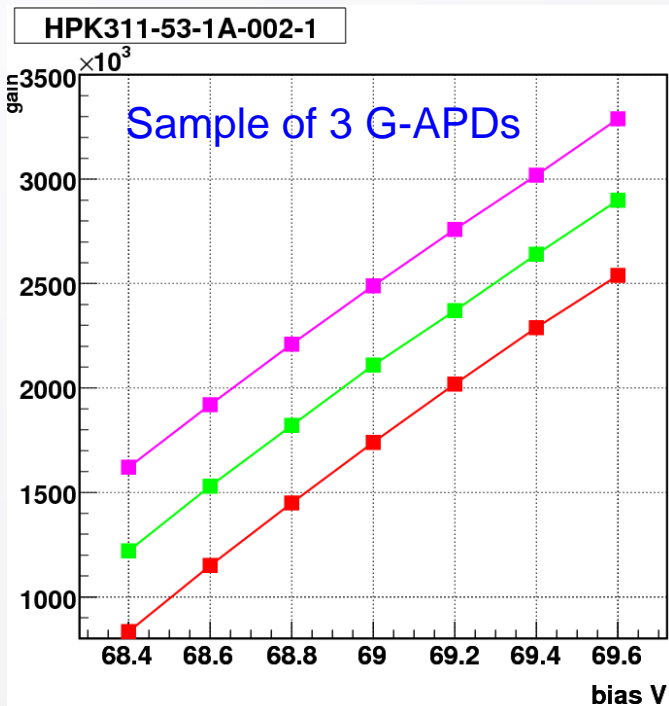


J. Haba, RICH2007

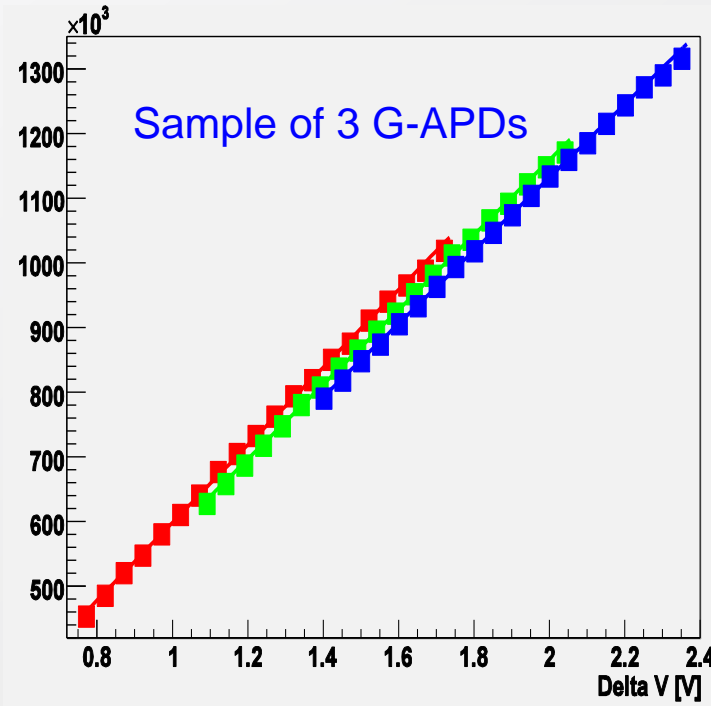


$$\begin{aligned}
 \text{Gain} &= Q / e \\
 &= I_{max} \cdot \tau / e \\
 &= (V_{BIAS} - V_{BD}) C_D / e \\
 &= \Delta V C_D / e
 \end{aligned}$$

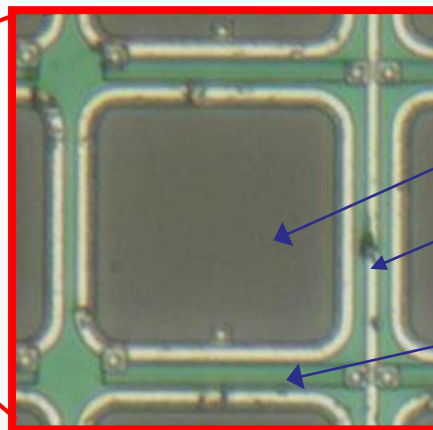
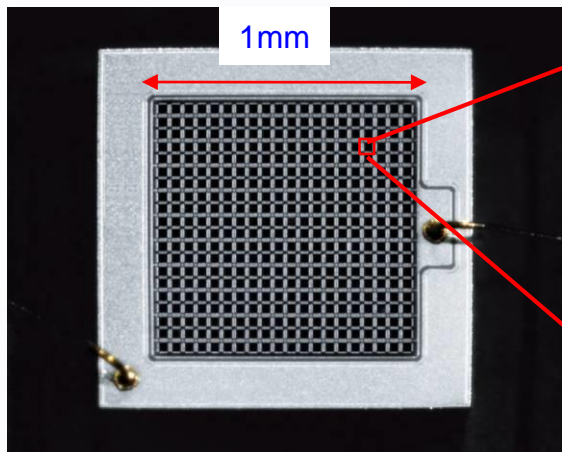
$G \sim 10^5 - 10^6$ at reasonable bias voltage
 (<100 V)



J. Haba, RICH2007



J. Haba, RICH2007



100 – several 1000 pix / mm²

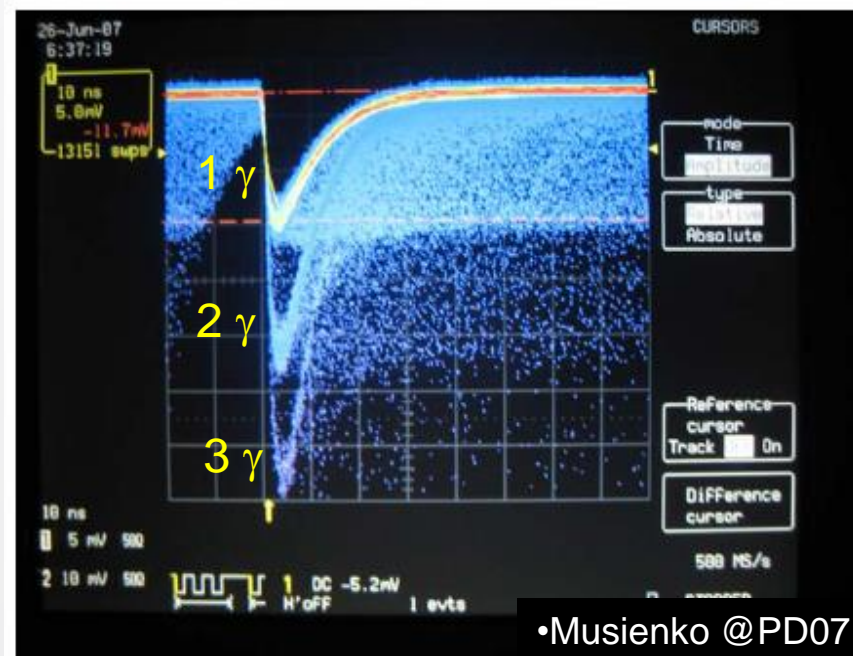
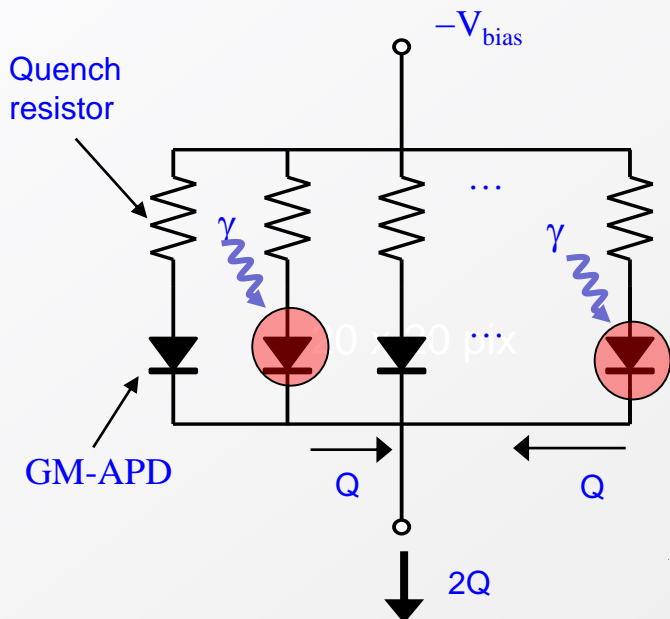
GM-APD

Bias bus

Quench resistor

Only part of surface is photosensitive!

Sizes up to 6x6 mm² now standard.



•Musienko @PD07

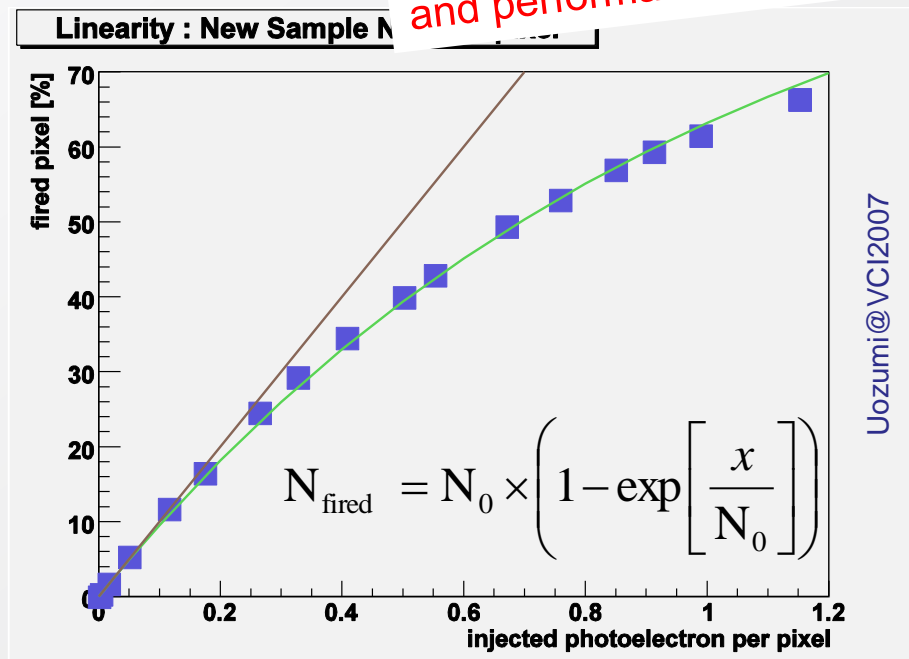
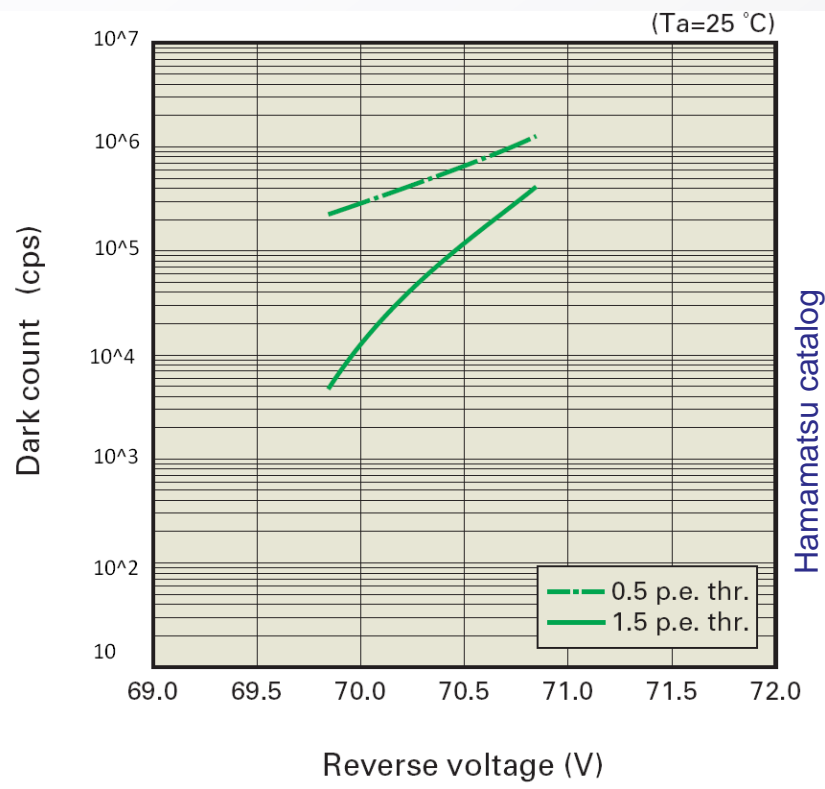
Quasi-analog detector allows photon counting with a clearly quantized signal



You cannot get "something for nothing"

- G-APD show dark noise rate in the O(100 kHz – MHz / mm²) range.
- The gain is temperature dependent O(<5% / °K)
- The signal linearity is limited
- The price is (still too) high

~10 producers are now in the market. Continuous improvement in technology and performance.



SiPM designs (just examples)

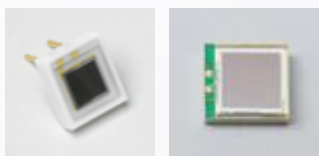
Hamamatsu HPK (<http://jp.hamamatsu.com/>)

25x25 μm^2 , 50x50 μm^2 , 100x100 μm^2 pixel size

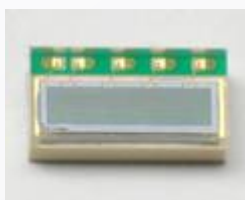
1x1mm²



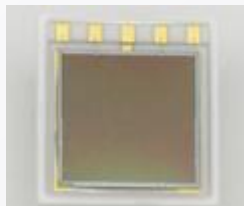
3x3mm²



Arrays



1x4mm²
1x4 channels



6x6 mm²
2x2 channels

FBK-IRST

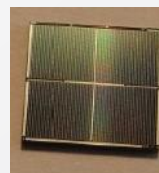
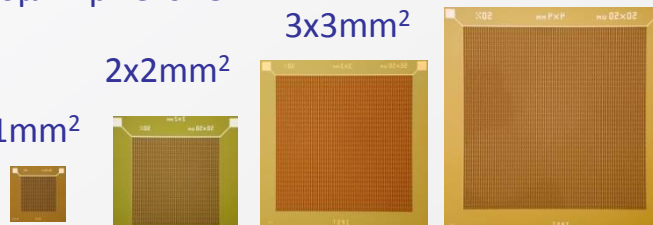
50x50 μm^2 pixel size

4x4mm²

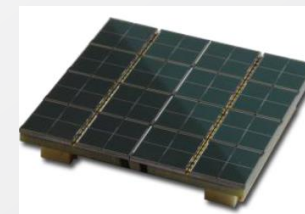
3x3mm²

2x2mm²

1x1mm²



4x4mm²
2x2 channels



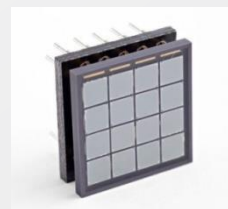
3x3 cm²
8x8 channels

SensL (<http://sensl.com/>)

20x20 μm^2 , 35x35 μm^2 , 50x50 μm^2 , 100x100 μm^2 pixel size



3.16x3.16mm²
4x4 channels



3.16x3.16mm²
4x4 channels

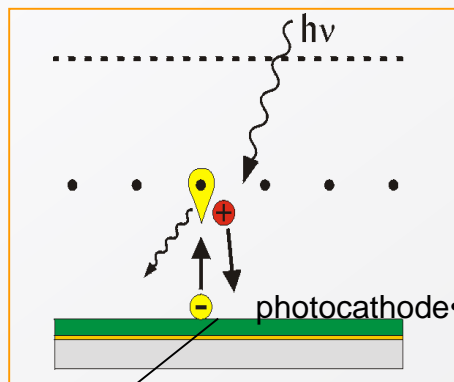
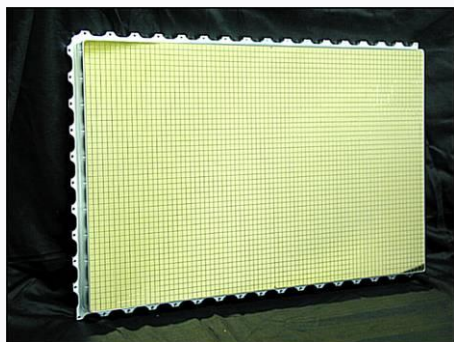


6 x 6 cm²
16x16 channels

Gaseous photodetectors: A few implementations...

Proven technology:

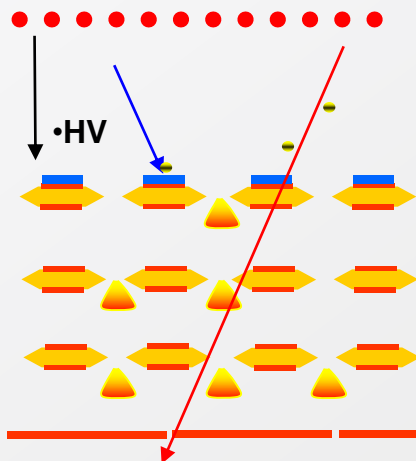
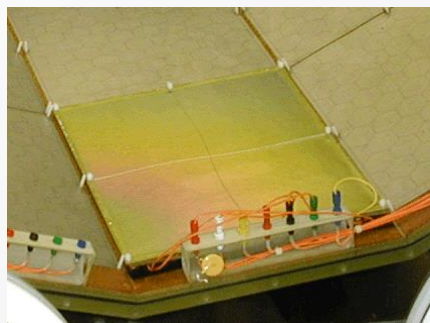
Cherenkov detectors in ALICE, HADES, COMPASS, J-LAB.... Many m² of CsI photocathodes



CsI on readout pads

Micro Pattern Structures (GEM) + CsI

HBD (RICH) of PHENIX.



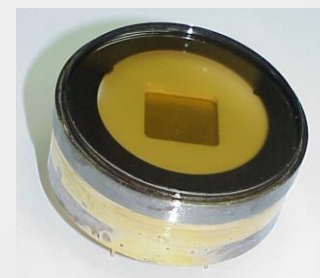
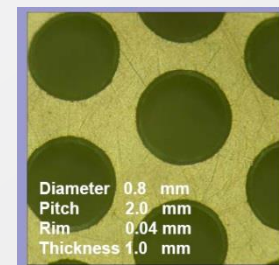
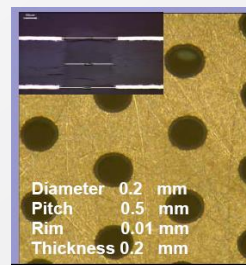
CsI on multi-GEM structure

R&D:

Thick GEM structures

Visible PC (bialkali)

Sealed gaseous devices



Sealed gaseous photodetector with bialkali PC. (Weizmann Inst., Israel)



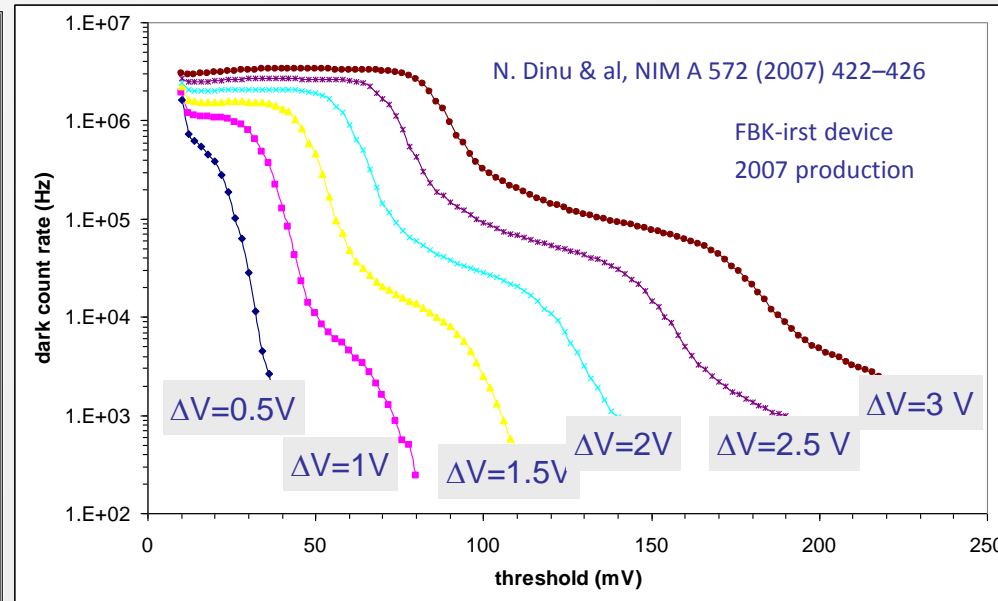
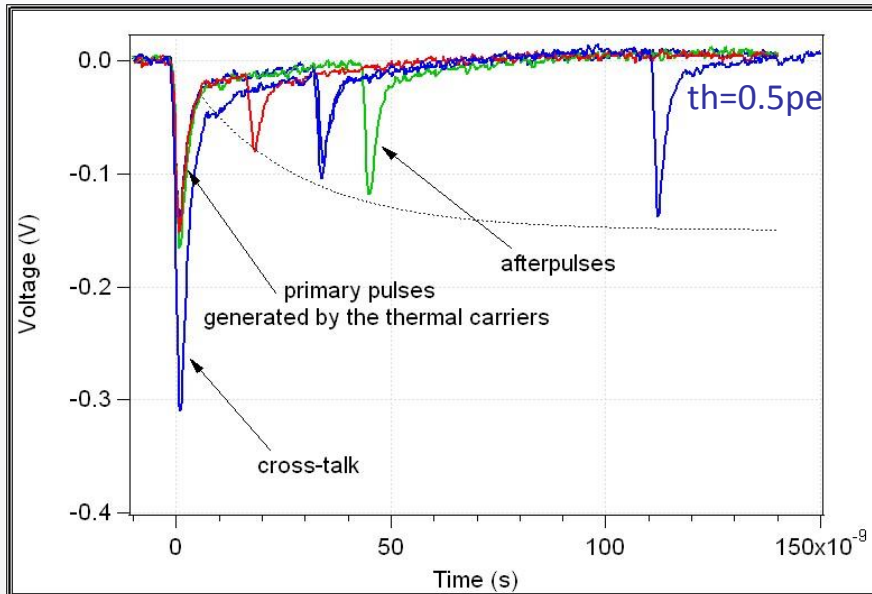
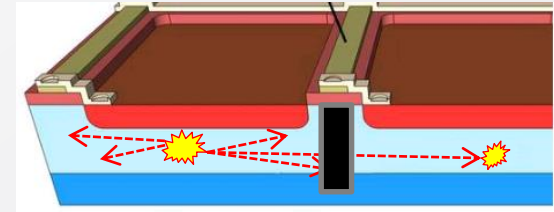
BACK-UP SLIDES

Dark counts due to ...

- **Thermal/tunneling** : thermal/ tunneling carrier generation in the bulk or in the surface depleted region around the junction
- **After-pulses** : carriers trapped during the avalanche discharging and then released triggering a new avalanche during a period of several 100 ns after the breakdown
- **Optical cross-talk**: 10^5 carriers in an avalanche plasma emit on average 3 photons with an energy higher than 1.14 eV (A. Lacaita et al. IEEE TED 1993). These photons can trigger an avalanche in an adjacent μ cell.

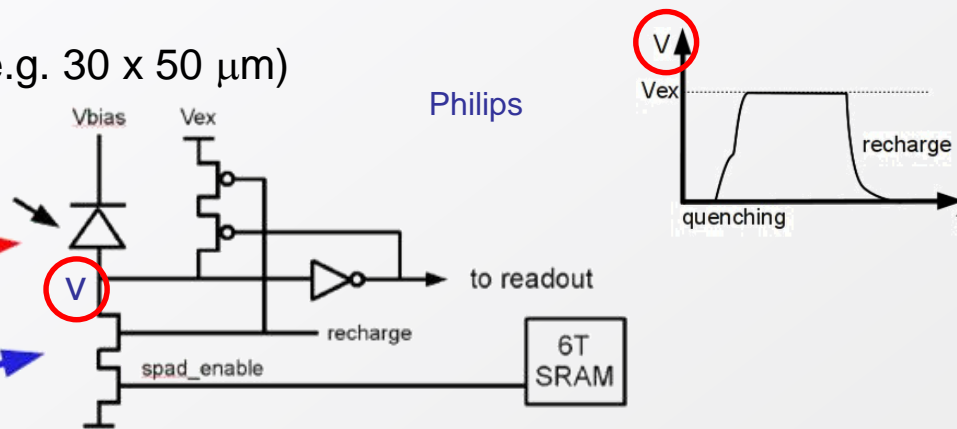
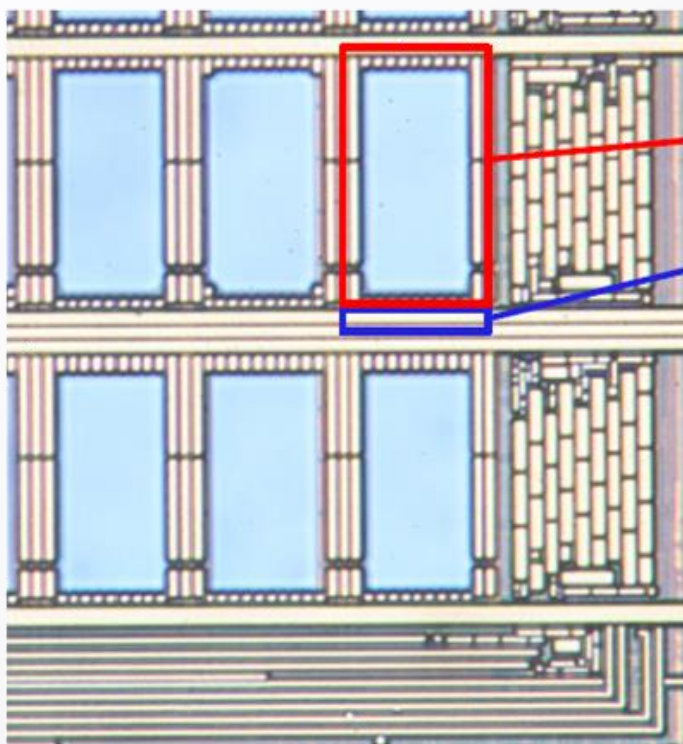
→ Limit gain, increase threshold

→ add trenches btw μ cells



Implementation of SiPMs in a CMOS process allows adding lots of functionality...

1 digital cell (area depends on type, e.g. 30 x 50 μm)



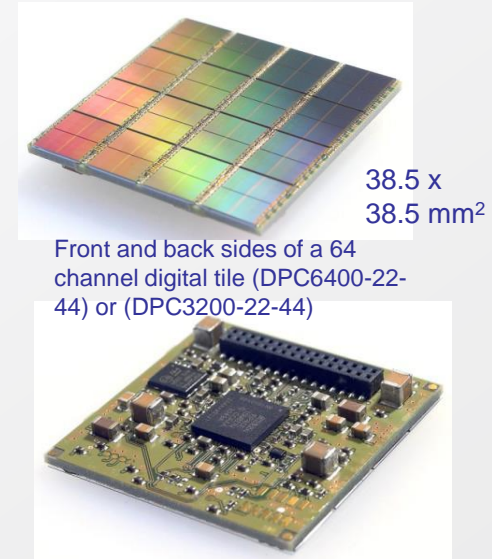
- Cell electronics area: 120 μm^2
- 25 transistors including 6T SRAM
- ~6% of total cell area
- Modified 0.18 μm 5M CMOS
- Foundry: NXP Nijmegen

Different from analog SiPMs: Upon the detection of a photon, the avalanche is actively quenched using a dedicated transistor, and a different transistor is used to quickly recharge the diode back to its sensitive state.

Compared to the analog technology, the digital one (offered by Philips) has a number of

advantages

- + Integration of bias supply, amp, TDC, counter...
- + Fast active quenching → no afterpulses
- + Possibility to de-activate noisy cells → potentially lower dark noise
- + Reduced sensitivity to voltage and temperature variations
- + Compactness
- + Possibility to add local intelligence



38.5 x
38.5 mm²

Front and back sides of a 64 channel digital tile (DPC6400-22-44) or (DPC3200-22-44)

Philips

... problems shared with analog

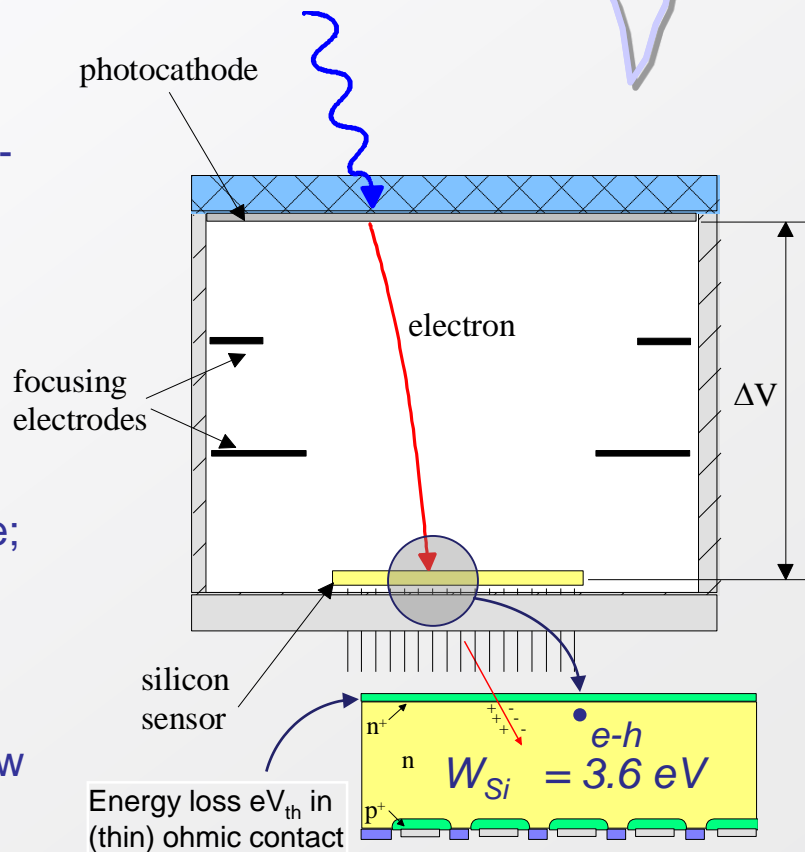
- High dark noise (a discharging cell doesn't know whether it is digital or analog)
- Signal saturation (limited number of cells)

... and also has some **drawbacks**

- The local electronics is a source of heat → cooling advisable
- The readout functionality is designed into the sensor. In case of mismatch with the needs, relatively expensive modifications of the sensor/FPGA may be required.

Basic principle:

- Combination of vacuum photon detectors and solid-state technology;
- Optical window, (semitransparent) photo-cathode;
- Electron optics (optional: demagnification)
- Charge Gain: achieved *in one step* by energy dissipation of keV pe's in solid-state detector anode; this results in low gain fluctuations;
- Encapsulation of Si-sensor in the tube implies:
 - compatibility with high vacuum technology (low outgassing, high T° bake-out cycles);
 - internal (for speed and fine segmentation) or external connectivity to read-out electronics;
 - heat dissipation issues;

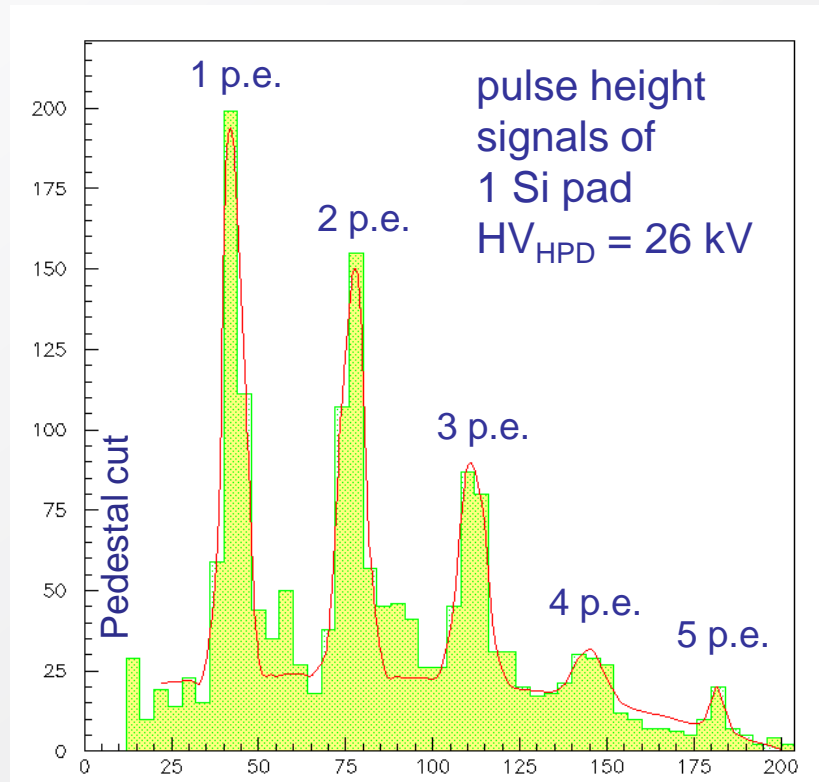


$$M = \frac{e(\Delta V - V_{th})}{W_{Si}} \quad \begin{array}{l} \Delta V = 20 \text{ kV} \\ \rightarrow M \sim 5000 \end{array}$$

$$\sigma_M = \sqrt{F \times M} \quad \begin{array}{l} F = \text{Fano factor} \\ F_{Si} \sim 0.1 \end{array}$$

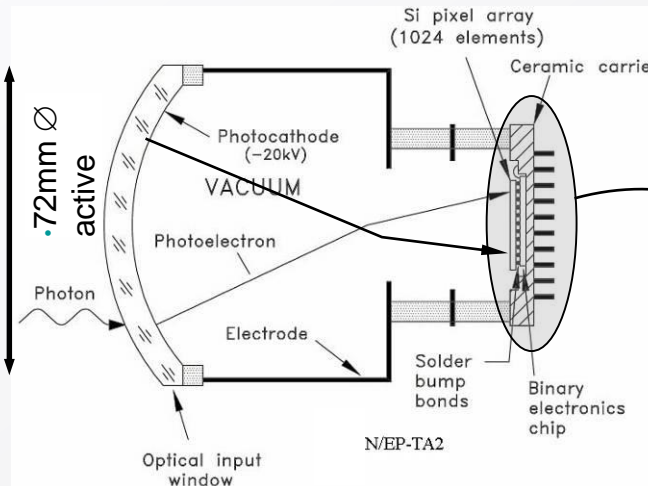


10-inch prototype HPD (CERN)
for Air Shower Telescope CLUE.

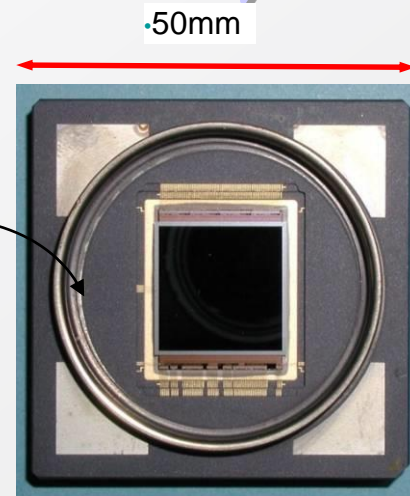


pulse height (ADC counts)

Photon counting. Continuum due to electron back scattering.

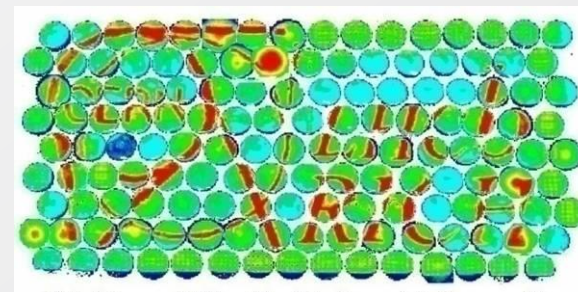


T. Gys, NIM A 567 (2006) 176-179



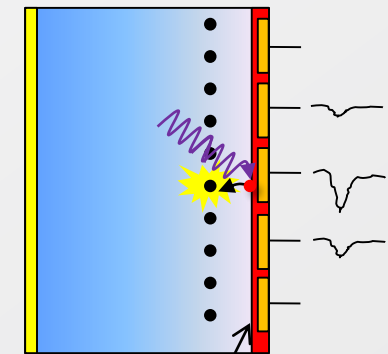
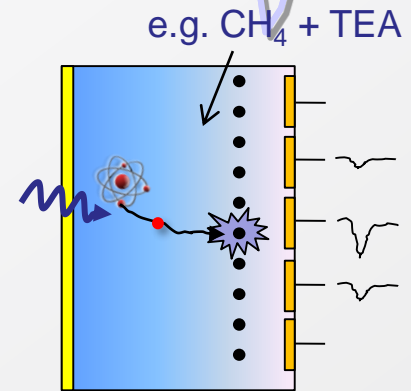
Pixel-HPD anode

- Cross-focused electron optics
- pixel array sensor bump-bonded to binary electronic chip, developed at CERN
- 8192 pixels of $50 \times 400 \mu\text{m}$.
- specially developed high T° bump-bonding;
- Flip-chip assembly, tube encapsulation (multi-alkali PC) performed in industry (VTT, Photonis/DEP)

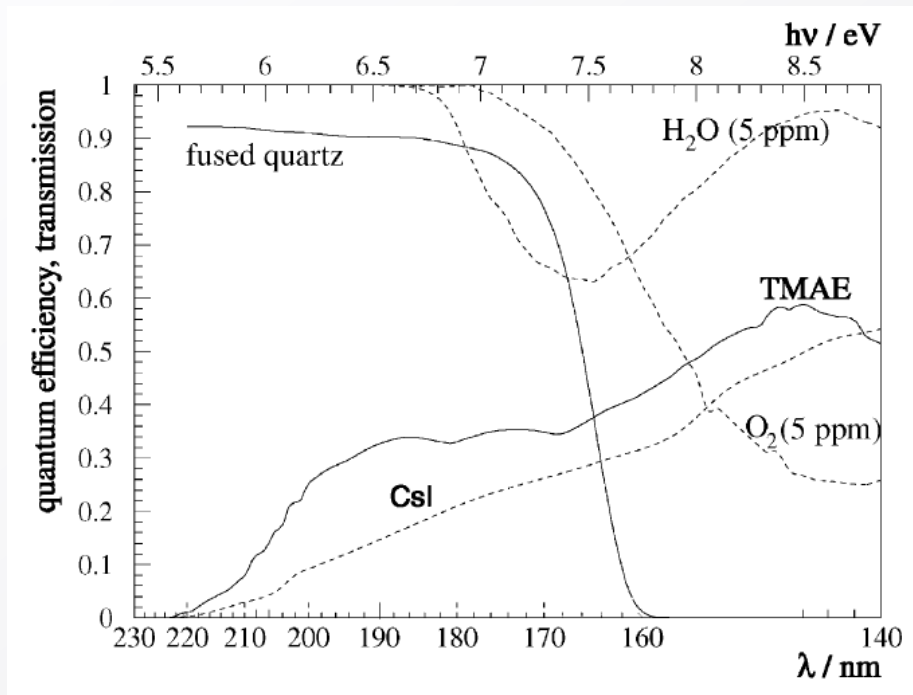


During commissioning:
illumination of 144 tubes by
beamer. In total : 484 tubes.

Principle: (A) Ionize photosensitive molecules, admixed to the counter gas (TMAE, TEA);
 or (B) release photoelectron from a solid photocathode (CsI, bialkali...);
 Then use free photoelectron to trigger a Townsend avalanche → Gain



Thin CsI coating on cathode pads



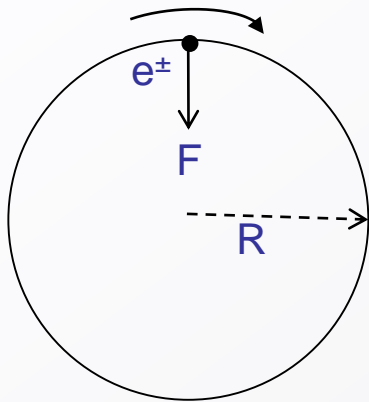
TEA, TMAE, CsI work only in deep UV region.

Bialkali works in visible domain, however requires VERY clean gases.

Long term operation in a real detector not yet demonstrated.

- Usual issues: How to achieve high gain (10^5) ? How to control ion feedback and light emission from avalanche? How to purify gas and keep it clean? How to control aging ?

Bremsstrahlung plays an important role in accelerators, but essentially only in circular e^\pm machines. Here it is called 'Synchrotron radiation'



Magnetic field forces particles on a circle \rightarrow permanent acceleration towards the centre of the circle.

Radiated power:

$$P_r = \frac{e^2 c}{6\pi\epsilon_0} \frac{1}{m^4} \frac{E^4}{R^2}$$

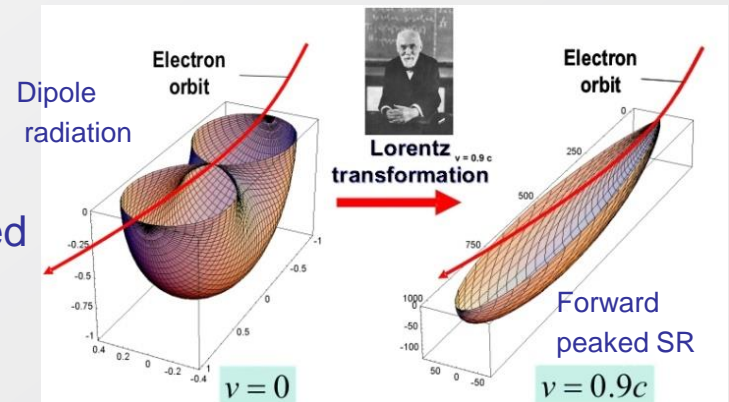
$$\frac{P_{r,e}}{P_{r,p}} = \frac{m_e^4}{m_p^4} \approx 1836^4 = 1.1 \cdot 10^{13}$$

Negative aspect: The radiated energy per turn can eat up the gained energy by acceleration and so limit the achievable energy. Famous example: LEP (e^+e^- collider).

$$\Delta E_{turn} = \oint P_r dt = P_r \frac{2\pi R}{c}$$

$$E_{LEP} \sim 100 \text{ GeV}. \quad R_{LEP} \sim 4300 \text{ m} \rightarrow \Delta E_{turn} \sim 2 \text{ GeV}$$

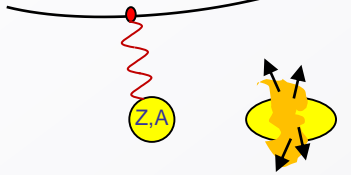
Positive aspect: The radiated energy is extremely forward peaked (Lorentz transformed) and can be used as very bright and intense photon source, e.g. for material studies. See e.g. ESRF (www.esrf.eu)



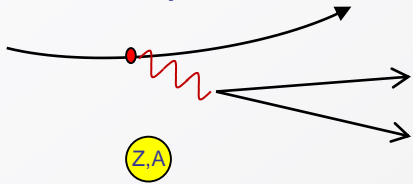
Muons interact electromagnetically (like the e^+, e^- , but due to its high mass, direct Bremsstrahlung ($\sim E/m^2$) is strongly suppressed.

There are other radiative processes

- Photo-nuclear interactions

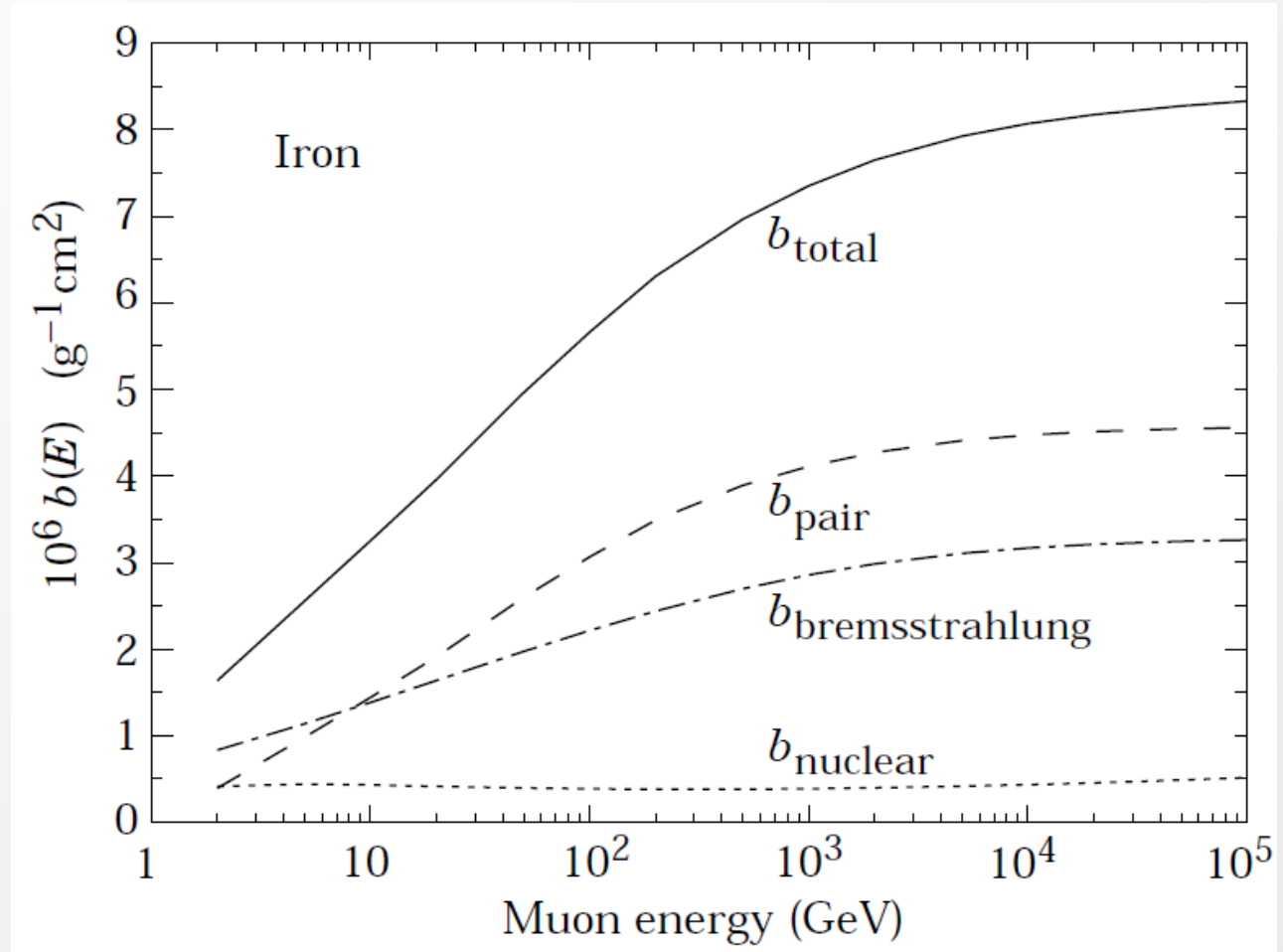


- Pair production



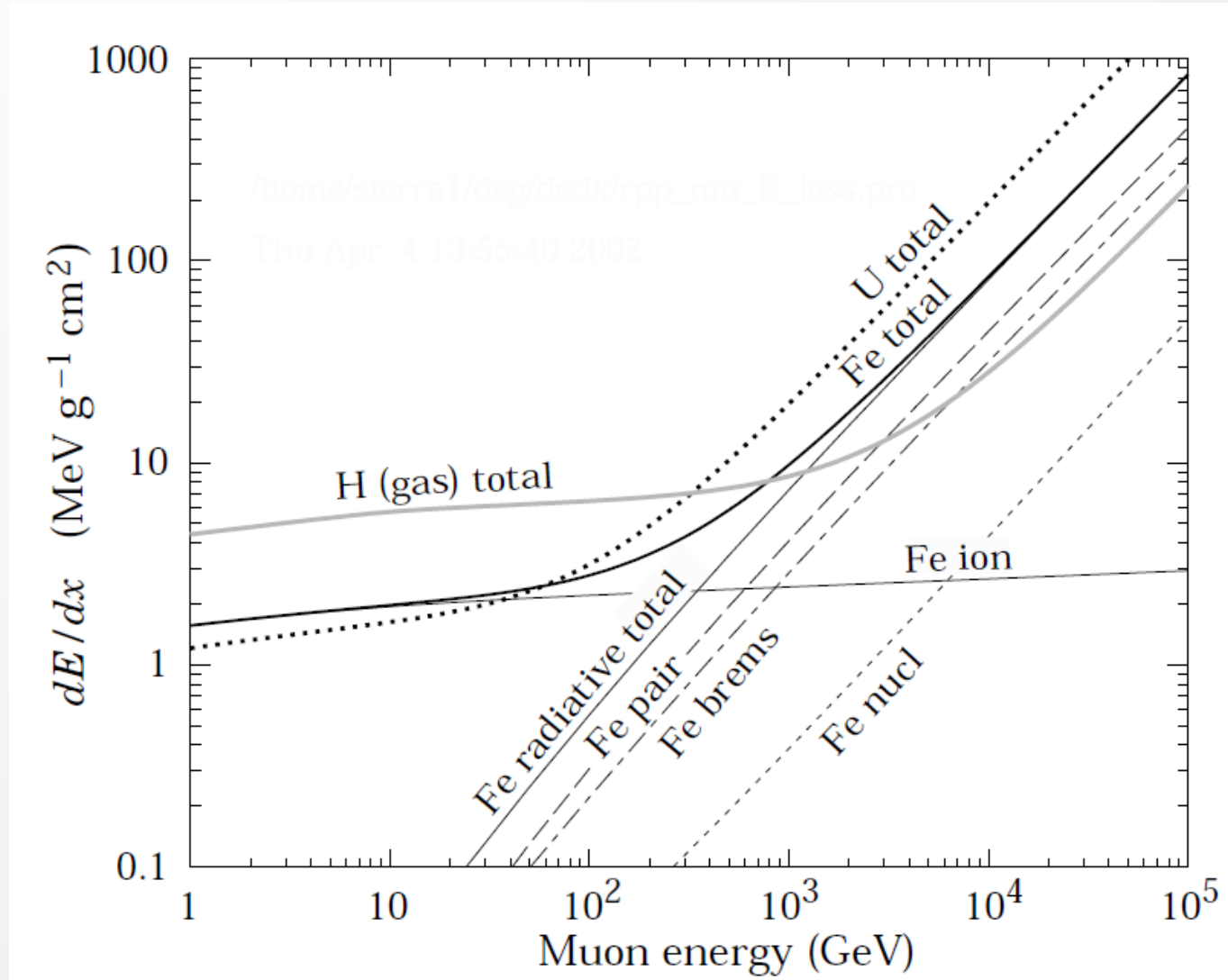
Like for Bremsstrahlung, they scale with E

$$\frac{dE}{dx} = b(Z, A, E_\mu) \cdot E_\mu$$

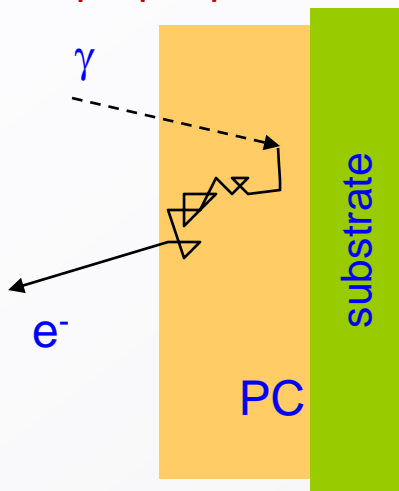


$$\frac{dE}{dx} = a + b \cdot E_\mu$$

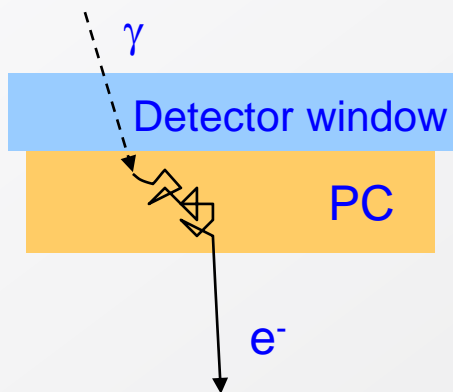
ionization radiative



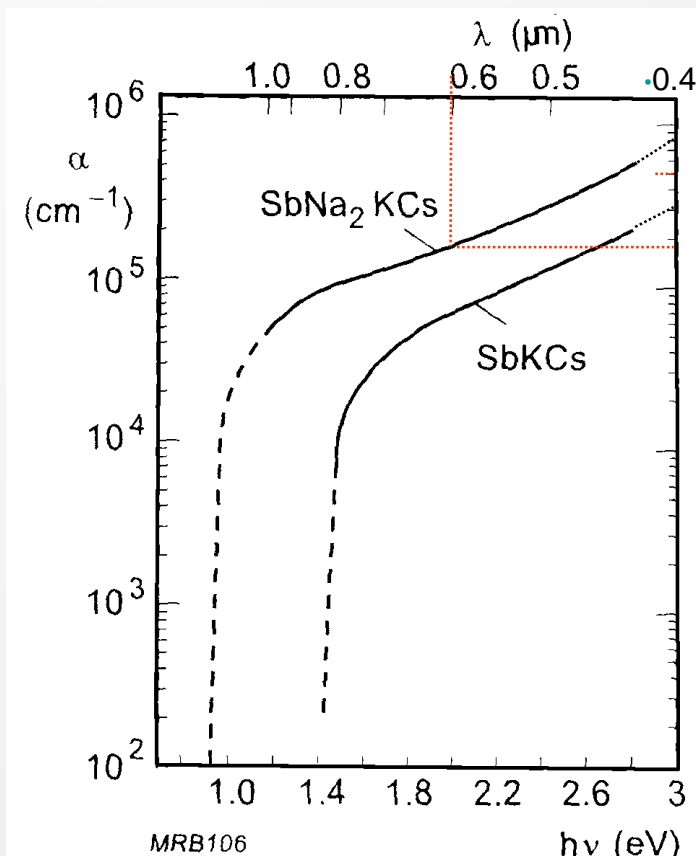
Opaque photocathode



Semitransparent photocathode



Light absorption in photocathode



$$\lambda_A = 1/\alpha$$

Red light ($\lambda \approx 600 \text{ nm}$)

$$\alpha \approx 1.5 \cdot 10^5 \text{ cm}^{-1}$$

$$\lambda_A \approx 60 \text{ nm}$$

Blue light ($\lambda \approx 400 \text{ nm}$)

$$\alpha \approx 4 \cdot 10^5 \text{ cm}^{-1}$$

$$\lambda_A \approx 25 \text{ nm}$$

Blue light is stronger absorbed than red light !

→ Make semitransparent photocathode just as thick as necessary!